Eur. Phys. J. H **37**, 413–458 (2012)
DOI: 10.1140/epjh/e2012-30017-2

THE EUROPEAN PHYSICAL JOURNAL H

Direct observations of galactic cosmic rays

Dietrich Müller[a]

Enrico Fermi Institute, The University of Chicago, 933 East 56th Street, Chicago, Illinois 60637, USA

Received 6 April 2012 / Received in final form 15 May 2012
Published online 25 July 2012
© EDP Sciences, Springer-Verlag 2012

Abstract. The mysterious "*radiation . . . entering our atmosphere from above*" discovered by Hess in 1912 is now known to be dominated by relativistic charged particles, mostly with energies in the GeV-range, but extending to energies higher by many orders of magnitude. As none of these particles can penetrate the earth's atmosphere without interaction, detailed studies of their composition and energy spectra require observations with high-altitude balloons or spacecraft. This became possible only towards the middle of the 20th century. The direct measurements have now revealed much detail about the Galactic cosmic rays below 10^{15} eV, but do not yet provide much overlap with the air-shower region of energies. A historic overview of the measurements is given, beginning with the realization that the majority of the cosmic rays are protons. The discovery and astrophysical significance of the heavier nuclei, and of the ultra-heavy nuclei beyond iron and up to the actinides, are then described, and measurements of the isotopic composition are discussed. Observations of the individual energy spectra are reviewed, and finally, the detection of electrons, positrons, and anti-protons in the cosmic rays, and the searches for exotic or unusual phenomena are summarized. Emphasis is given to the fact that all of these discoveries have become possible through the evolution of increasingly sophisticated detection techniques, a process that is continuing through the present time. The precise knowledge of the abundance distributions of the elements in the cosmic rays and of their isotopic composition permits a comparison with the "universal abundance scale" and provides strong constraints on the origin of the cosmic-ray material in the interstellar medium. "Clock-isotopes" reveal the time history of the particles. The shapes of the energy spectra of the individual cosmic-ray components are related to evolving ideas about particle acceleration and propagation in the Galaxy. In conclusion, prospects for future work are briefly discussed.

1 Introduction: Going above the atmosphere

This report will attempt to present a historic review of the direct measurements of the charged Galactic cosmic rays. Neutral radiations such as gamma rays or neutrinos

[a] e-mail: dmuller@uchicago.edu

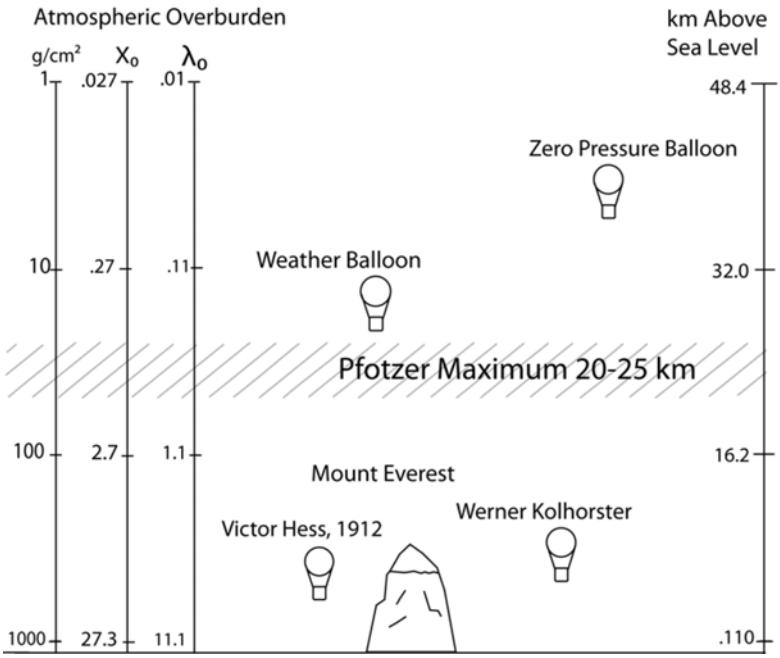

Fig. 1. Float altitude and atmospheric overburden of balloons. Maximum secondary particle production occurs at the "Pfotzer maximum" (see also Fig. 3).

will not be included, and energetic particles of Solar or interplanetary origin are also beyond the scope of this discussion. We know now that the components of Galactic cosmic rays are mainly protons, but also include the nuclei of all the heavier elements, from helium to the actinides, as well as electrons, positrons, and anti-protons. Cosmic rays cover a very wide range of energies. Up to at least 10^{16} eV *per particle*, they appear to be created predominantly in the Galaxy, but at the highest energies, extending to more than 10^{20} eV, extragalactic contributions cannot be ruled out. None of the cosmic-ray species at any energy can penetrate the Earth's atmosphere without interaction. As illustrated in Figure 1, the atmosphere, with a mass overburden of 1033 $\mathrm{g\,cm^{-2}}$ under normal conditions at sea-level, represents a formidable obstacle, equivalent to 11.5 proton interaction lengths (λ_0), or to 28 radiation lengths (X_0). Hence, just the products of multiple nuclear and electromagnetic interactions, i.e., mostly electrons and muons (and photons and neutrinos) may arrive at sea-level, providing only limited and indirect information about the properties of the primary cosmic rays.

To observe the primary cosmic rays directly, one must place a detector at an altitude where the remaining mass overburden is just a fraction of an interaction length, or better, a fraction of a radiation length. This is a major technological challenge and was beyond reach during the early decades of cosmic-ray research. The spectacular balloon flights of Hess and Kolhoerster in 1912–1913, reaching altitudes up to about 8 km, or about 350 $\mathrm{g\,cm^{-2}}$ ($3.9\lambda_0$ or $9.6X_0$), could not detect the primary particles. The increase in the secondary ionization density with altitude was the telling feature that led to the conclusion that the primary cosmic rays originated above the atmosphere.

Because of this atmospheric barrier, initial cosmic-ray research was largely concerned with studies of the nature and interactions of the secondary particles in the atmosphere. The dramatic discoveries of such studies provided the foundation for modern elementary particle physics. However, information about the properties of

the primary radiation was scarce and controversial. For instance, there was notorious disagreement between Compton and Millikan in the 1920's and early 1930's about the primary cosmic rays being charged particles or γ-ray photons. This controversy was decided in favor of Compton through the discovery of the "latitude effect" [Clay 1932; Compton 1932]: the sea-level particle intensity depended on geomagnetic latitude. Hence, the primary "rays" must be affected by the earth's magnetic field., and therefore, had to be charged particles.

Also in the early 1930's, the "East-West effect" was discovered [Alvarez 1933; Johnson 1933]: it appeared that the atmospheric secondary particles on ground partially "remembered" the direction of incidence of their primary parents, and that more particles arrived from westerly directions than from the east. If this effect is caused by the azimuthal variation of the rigidity cutoff of the primary particles, it indicates that these are mostly positively charged. It seems obvious then to suspect that the primaries might be dominated by protons. However, this conclusion was difficult to prove at the time, because it was not understood how nuclear interactions of protons could generate the observed secondary particles in the atmosphere. To quote from Bruno Rossi, who had made the first attempt to observe the East-West asymmetry in 1931:

> *"It was thus clear that a portion, possibly all, of the primary cosmic radiation consisted of positively charged particles. This was a most unexpected result, for the common belief among proponents of the corpuscular hypothesis had been that the primary cosmic radiation consisted of electrons. Had the east-west effect been discovered one year earlier, we would have concluded that cosmic rays must be protons or heavier nuclei, since these were the only positively charged particles known at the time. And it so happens we would have been right. But in 1932 a new positive particle had been discovered – the positive electron or positron. Thus we had to leave the question of the nature of primary cosmic rays in abeyance until new evidence developed." [Rossi 1964].*

To reach elevated altitudes, balloons were used. Initially, these consisted of rubberized material, forming a closed shell filled either with town gas or with hydrogen, and carrying a gondola with the observer and his equipment onboard. The total mass of the arrangement was too large as to permit float altitudes above about 10 km. Modern airplanes, which later also carried cosmic-ray detectors, usually do not reach altitudes that are significantly higher than those of the early balloon flights.

Beginning in the 1930's, two developments led to progress: first, light-weight detectors became available, and second, automated data recording (aided by telemetry for electronic detectors) eliminated the need for dangerous man-tended payloads. This made possible the exposure of instruments on rubber balloons which were readily available for weather observations, and which could obtain maximum altitudes of more than 30 km. However, flight durations were short (typically less than an hour), because the balloon would burst due to internal over-pressure, hastened by degradation of the material in the solar ultra-violet radiation. Typical detector arrangements, for instance designed by Vernov, one of the pioneers in this research in Russia [Vernoff 1934], would include Geiger-Müller counters in coincidence. Later, emulsion stacks were also widely used. These flights made possible the first glimpses at the primary cosmic rays, and were therefore conducted at many places during the 1930's and 1940's. Figure 2 shows launch activities on the campus of the University of Chicago in 1948. Here, the Football arena called Stagg's Field[1] was used as a launch site by a group of scientists including Arthur Compton, Marcel Schein, and John Simpson.

[1] The same location where the West Stands, seen in the background, housed the first nuclear pile constructed by Fermi and collaborators in 1942.

Fig. 2. Launch of payloads carried by weather balloons in 1940's. The launch site is Stagg's Field, the football stadium at the University of Chicago. Note that the instruments had to be light-weight, and could be easily held and manipulated for launch by hand, even if multiple balloons were used to carry a single payload (from Marcel Schein papers; special collections at University of Chicago Libraries).

Finally, technological advances after World War II led the way to new and capable platforms for direct and definitive observations of the primary cosmic rays before they enter the atmosphere. Upon the initiative of van Allen, V-2 rockets captured in Germany were instrumented with Geiger-Müller counters and provided the first intensity profiles of cosmic-ray particles well above the atmosphere. Figure 3 shows an example of such measurements [van Allen 1948]: one notices a steep increase in intensity with altitude, the onset of which was first discovered by Hess in 1912, until a maximum of secondary particles is reached around 20 km above ground (the "Pfotzer maximum", discovered by [Pfotzer 1936]), followed by a decrease until a steady plateau is measured above 50 km. Presumably, this plateau represents the primary intensity

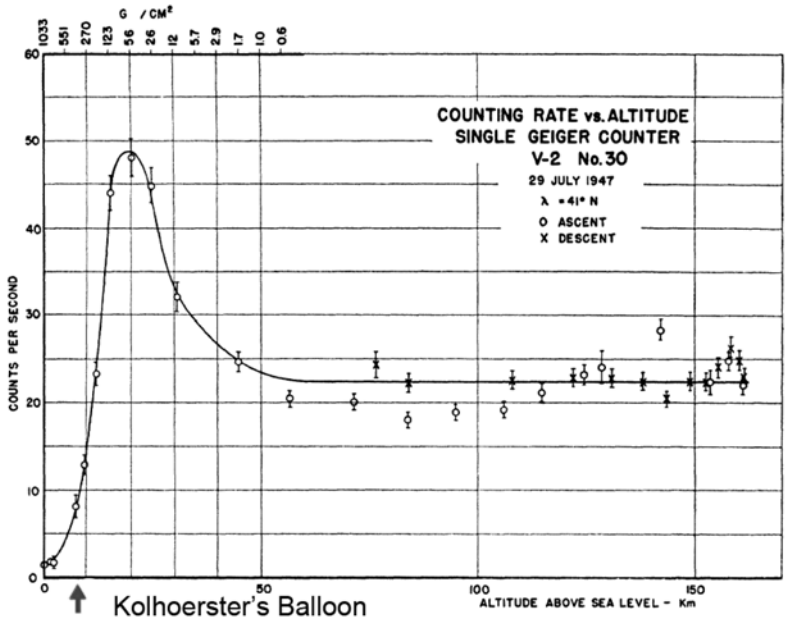

Fig. 3. Count rate of particle detector vs. altitude, measured in ballistic rocket flight in 1948. The arrow indicates the elevation of Kolhörster's balloon flight in 1912/1913 (figure from [van Allen 1948]).

arriving from the Galaxy[2]. While such measurements were severely limited by the short duration of just a few minutes of a ballistic flight above the atmosphere, they provided the technological basis for satellite observations in later decades.

In the late 1940's, the development of a new type of balloon commenced. These "Zero-Pressure" balloons are made of very thin (of order 10 μm) polyethylene films, reinforced with longitudinal "load tapes" to carry the payload, and may reach float altitudes between 30 and 45 km (corresponding to residual atmospheric overburdens between 12 and 1.5 g cm^{-2}). The balloons are filled with helium or hydrogen, but have openings at the bottom to ensure pressure equilibrium with the outside atmosphere. Thus at launch, the balloon appears to be only partially inflated, but the gas will expand on ascent until nearly spherical shape (with a diameter that may exceed 100 m) is attained at float altitude, with minimum stress on the material due to differential pressure. Ironically, this technology was developed for reconnaissance flights by the US Navy during the Cold War, just as the balloons used by Victor Hess before World War I had been designed for military purposes.

Zero-pressure balloons have been the work horse for numerous cosmic-ray observations until the present time. They can lift substantial payload masses, of the order of several tons. A typical flight duration may not exceed one or two days, as the balloon volume shrinks during a day-night transition due to the decrease in temperature. The balloon then tends to become unstable unless significant amounts of ballast are released. However, beginning in the 1990's, this limitation was overcome with "long-duration balloon flights (LDB)" circling the Antarctic continent. In such flights, the permanent sunshine and the circum-polar stratospheric wind pattern of local summer

[2] Later, additional intensity variations at greater altitude were discovered in satellite observations and were associated with trapped particle populations in the "radiation belts" named after van Allen.

Fig. 4. Launch of a cosmic-ray detector with zero-pressure balloon for long-duration flight in Antarctica. The payload is quite large and is put in position with a special heavy-duty launch vehicle. Sizeable solar photovoltaic arrays are needed to provide power during the flight. Data and command communication during flight is usually provided via a satellite link, for instance NASA's TDRS network [Launch of BESS-Polar, 2004; from BESS website].

are utilized to extend the flight time. Launched from the McMurdo Station, a single circular pass around the pole may take up to two weeks, and total flight durations of several weeks are now routinely achieved. Figure 4 shows a photograph of an Antarctic balloon launch. Circum-polar LDB flights are also possible during summer in the Northern hemisphere, but are not presently conducted for geo-political reasons.

Finally, new materials are currently developed that permit the construction of large pressurized balloons of fixed volume ("super-pressure balloons") which could afford ultra-long flight durations with fewer restrictions on location or time of year.

While balloon flights represent a relatively economical method to carry scientific equipment to the top of the atmosphere, cosmic-ray detectors have also been flown on spacecraft since the beginning of the space age. The exposure times may then measure in years. Naturally, the cost of such instruments is high, and weight restrictions may be severe unless very large launch vehicles are available, or the space shuttle and space station are utilized. The advantages of spacecraft are that the residual atmospheric overburden is truly zero, and that, either with polar orbiting satellites or with deep space probes, effects caused by the Earth's magnetosphere can be overcome. These features are important for measurements at low particle energies (below the GeV region).

2 Composition and energy spectra of cosmic-ray nuclei

2.1 Cosmic rays from supernovae?

There are two major and interrelated questions about the primary cosmic rays: the first is about the nature and composition of the primary particles, and a historical

account of relevant observations will be given in the following chapters. The second question refers to the origin and acceleration of the cosmic-ray particles. This question remains a subject of ongoing research, with answers developing as more refined measurements become available. Already Hess suggested that the cosmic rays must come from greater distances than the Sun because no diurnal variations in intensity, nor a reduction during a solar eclipse were observed [Hess 1912]. While there are energetic particles generated in Solar flares, the now generally accepted view agrees with Hess' suggestion: the bulk of the primary cosmic rays is thought to come from acceleration sites farther away in our Galaxy. However, the possibility of a solar origin was discussed for a long time, for instance by Teller, and Alfven [Alfven 1950; Richtmyer 1949].

During the 1930's, the phenomenon of supernovae (SN) was first described by Baade and Zwicky, and it was realized that enormous amounts of energy could be released in a SN explosion. Far ahead of their times, Baade and Zwicky then suggested that SN explosions could supply the energy required for the generation of cosmic rays [Baade 1934a]. Baade and Zwicky did not restrict their suggestion to SN just in our Galaxy but assumed that SN in distant galaxies would also contribute to the cosmic-ray intensity observed near Earth. They could not propose a mechanism of energy transfer to comic-ray particles during the explosion, and they did not consider the crucial role of magnetic fields in the acceleration and propagation of energetic particles. However, they proposed [Baade 1934b] that the seed material for cosmic rays was stellar gas released in the explosion, and that therefore the cosmic rays should consist of protons and heavier ions. It took nearly two decades until this prediction was indeed on solid observational ground.

It is interesting to compare the SN hypothesis with presently known numbers: the energy density of cosmic rays in the Galactic disk (with a volume of about 10^{67} cm^3) is of the order of 1 eV cm^{-3} (1.6×10^{-12} erg cm^{-3}), and the particles are confined to the Galaxy for about 10^7 years (see Sect. 2.6). Thus, the cosmic-ray luminosity of the Galaxy must be about 5×10^{40} erg s^{-1}, and indeed, a very powerful source mechanism is required. If there are 3 explosions per century, with a typical energy release of 10^{51} erg for a type II SN, about 5% of the total energy of the explosions would be needed to generate the cosmic rays.

2.2 Protons in the cosmic rays

As mentioned above, geomagnetic effects had indicated that the majority of the primary cosmic rays are positively charged particles, and some observers suggested that positrons, rather than protons, should be a major component in the primary radiation. This question could find a definitive answer when instrumentation with sufficient particle-identification power could be carried to high altitudes $\gtrsim$30 km. Measurements were made at a number of institutions in the 1940's, with the most definitive observations coming from balloon flights conducted by Marcel Schein and colleagues [Schein 1941]. Their instrumentation consisted of arrangements of Geiger-Müller counters, interspersed with lead absorbers to reject electrons. No primary electrons were observed, and the particles were found to be "penetrating", and to be attenuated in the atmosphere as one might expect for protons. Figure 5 shows this result as reported in 1941. In 1948, Hulsizer and Rossi [Hulsizer 1948] concluded from balloon flights with a lead-shielded ionization chamber that less than 1% of the proton intensity in the GeV region could be attributed to electrons or positrons. However, this was an upper limit, and not until the 1960s were electrons indeed detected in the primary cosmic radiation (see Sect. 3.1).

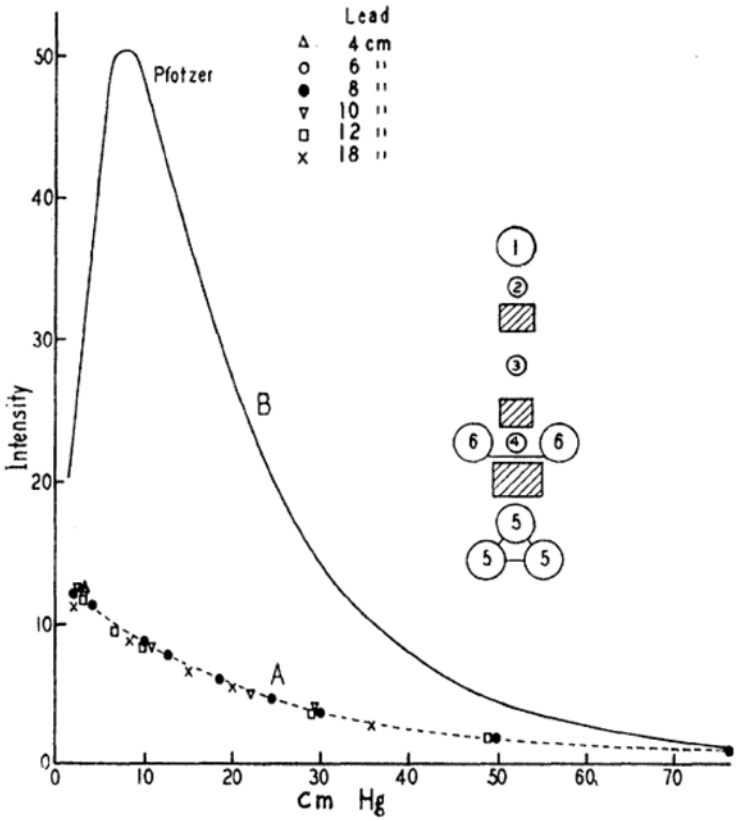

Fig. 5. Intensity of vertical cosmic ray particles penetrating through several radiation lengths of lead vs. atmospheric depth in cm of Hg. The particles are identified by coincidences between Geiger-Müller tubes 1,2,3,4; or 2,3,4,5 (Curve A). Curve B is the total intensity including secondary particles as measured by Pfotzer (see also Fig. 4) (figure from [Schein 1941]).

Not only did it become clear that the primary cosmic rays are dominated by protons, it also was inferred from observations of air showers at sea-level and mountain altitudes [Hilberry 1941] that the differential energy distribution of primary cosmic rays follows a power law $\propto E^{-\alpha}$, with index $\alpha \approx 2.75$.

These two observations were combined by Enrico Fermi with refined knowledge about the interstellar magnetic fields, to develop his famous theory of cosmic-ray acceleration in the Galaxy [Fermi 1949]. Contrary to the proposal by Baade and Zwicky, this theory does not propose localized acceleration sites like supernovae, but involves repeated interactions of charged particles with large-scale magnetic field irregularities moving with speed V in the Galaxy. The interactions are stochastic and therefore lead to power-law energy spectra, but the mechanism is not very efficient, as the average energy gain per collision is proportional to just $(V/c)^2$ ("second order Fermi acceleration"). According to Fermi, this mechanism could provide a satisfactory explanation for the observed intensity of protons. However, Fermi also noted that heavier nuclei could not be accelerated in this fashion because ionization energy losses would not permit the "injection" of these particles into the cosmic accelerator. Similarly, for electrons (if there were any in the cosmic rays), energy losses would exceed the energy gained in the process.

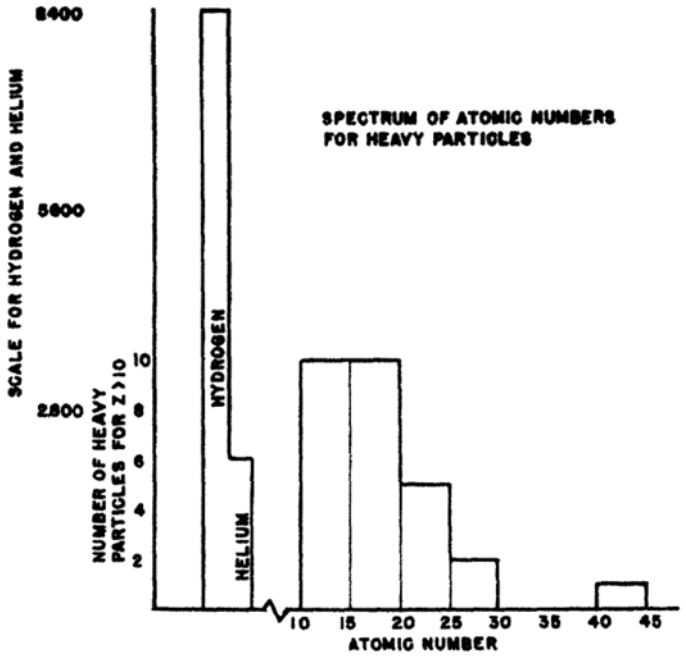

Fig. 6. Charge distribution of heavy nuclei discovered in 1948 (figure from [Freier 1948b]).

Unfortunately for the theory, just about at the same time, the first definitive observations of heavy nuclei in the cosmic rays were made (see Sect. 2.3). Hence, the Fermi-theory in the original form was insufficient as a likely mechanism for the origin of cosmic rays. It took another 30 years, and many more detailed observations, until a mechanism of "first order Fermi acceleration" was developed which now is more broadly accepted. This process, known as "shock acceleration", also reconciles the Fermi mechanism with the supernova hypothesis proposed by Baade and Zwicky (see also Sect. 2.7.2).

2.3 Heavy nuclei

New discoveries in cosmic-ray physics have always been tied to new observational techniques. In the 1940's, most important advances came from the development of the nuclear emulsion technique. Details on the history of the technique, and a discussion of early work, for instance by Marietta Blau and Hertha Wambacher in Austria, and the contributions of the Bristol group, can be found in [Powell 1959]. It was now possible to visualize the track of a charged particle through the emulsion and to measure the ionization density which is proportional to Z^2/v^2, where Z is the nuclear charge of the particle, and v its speed. One could also observe individual δ-rays along the particle track, and with a stack of emulsions, one could detect the slowing-down of sub-relativistic particles due to ionization energy losses.

This technique was applied in balloon borne observations in the late 1940's at altitudes corresponding to about 25 $\mathrm{g\,cm^{-2}}$ or less, and led to the discovery of the heavier elements, from alpha-particles to iron nuclei and beyond, in the cosmic rays. The pioneering measurements were made by a collaboration between the University of Minnesota and Rochester University, using nuclear emulsions, combined with a cloud chamber [Bradt 1948; Freier 1948a;b], and were soon confirmed by other observers, e.g. Pomerantz and Hereford [Pomerantz 1949]. Figure 6 shows an initial charge histogram

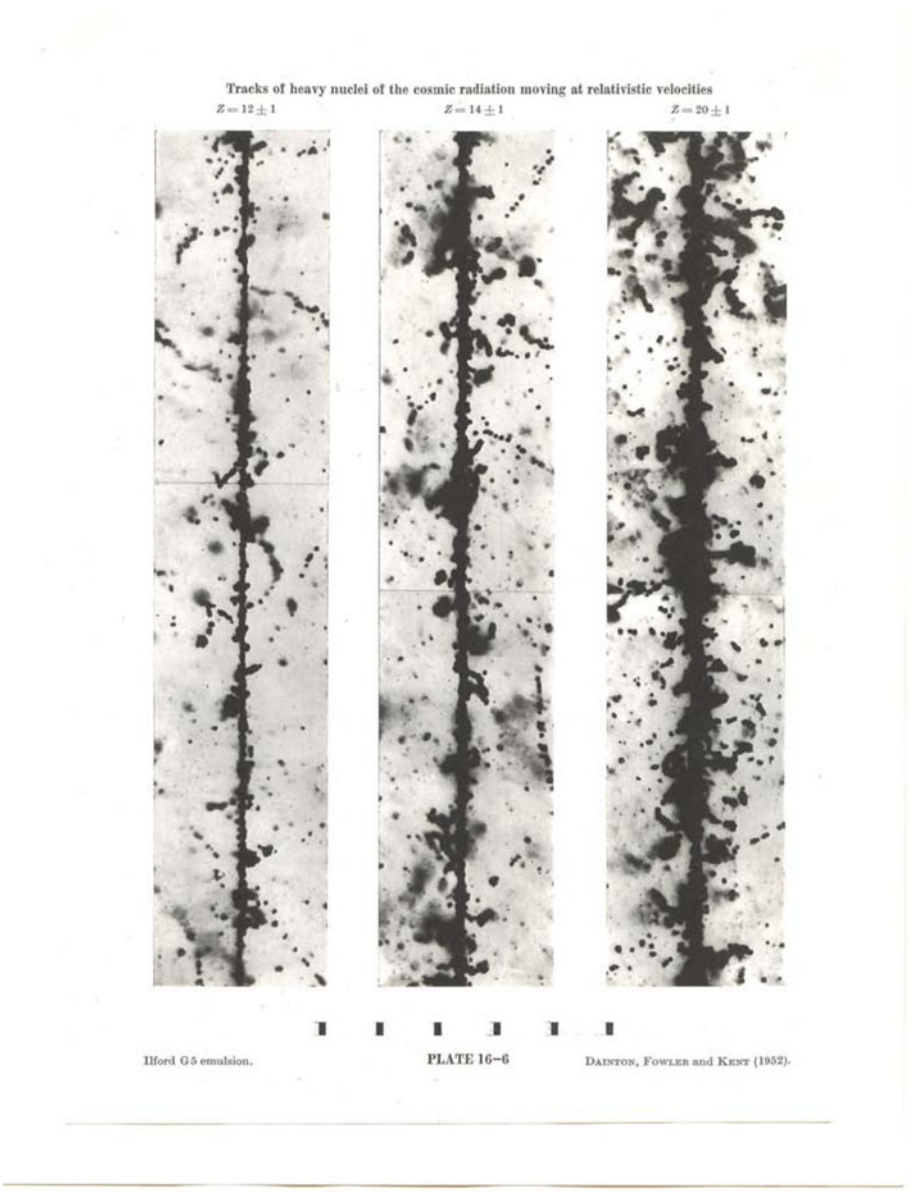

Fig. 7. Photomicrographs of the tracks of 3 relativistic nuclei with charge numbers 12, 14, and 20 in Ilford G5 emulsion. Figure based on observations of Dainton, Fowler, and Kent (1952), reproduced in [Powell 1959]. Scale: distance between markers corresponds to 10 μm.

from the work of Freier et al., and Figure 7 shows the tracks of three relativistic nuclei as observed by the Bristol group (quoted by [Powell 1959]).

While the resolution in elemental charge in the early observations was still crude, these measurements had very important implications: first, it became obvious that cosmic rays could not have cosmological origin. The heavy elements in the cosmic

rays must have been produced by nucleosynthesis in stars, and subsequently injected into some kind of a cosmic accelerator. Second, as mentioned, an acceleration process other than the Fermi mechanism in its original form was required to account for the heavy nuclei.

Subsequent to this discovery, the obvious experimental challenge was measurements that could determine the relative abundances of the individual cosmic-ray components with good accuracy, and that could measure the individual energy spectra over a wide range. This challenge was met with a variety of experimental techniques and in numerous observations both on balloons and with spacecraft, some extending into the present time. We will visit some of this work in the following chapters. Many groups were involved, and it is not possible to quote all individual contributions. However, it is to be noted that these investigations represented a truly international effort, with instruments developed at a number of individual institutions in the US, and throughout Europe and the Soviet Union, as well as in India and in Japan.

2.4 Details of the elemental composition

The identification of a cosmic-ray nucleus requires the measurement of two parameters, the elemental charge Z, and the kinetic energy E (or velocity v, or momentum p)[3]. The isotopic identification, i.e. determination of the mass number A, was not possible in the initial observations, and will be discussed in Section 2.6. Nuclear emulsions permit highly precise measurements, but require tedious readout techniques. This disadvantage could be overcome with solid-state detectors with electronic read-out that began to become available in the 1960s. Typically, a cosmic-ray telescope would consist of one or several thin solid state detectors measuring the specific ionization, dE/dx, followed by a thick detector in which the particle stops and deposits a signal proportional to its total remaining energy. This combination, known as "dE/dx vs. E technique", has been in use until the present time for detectors of relatively small area. Figure 8 shows an early instrument of this type, designed by Simpson and colleagues [Garcia-Munoz 1973]. The requirement that the particle stops in the detector, limits this technique to fairly low energies, typically up to a few hundred MeV amu^{-1}. Therefore, this approach has been mostly used in observations on spacecraft.

At highly relativistic energies, a cosmic-ray nucleus cannot be stopped in a detector within reasonable mass limits, and the low intensity calls for instruments with large areas, of the order of square meters. Therefore, sheets of plastic scintillators or gas-proportional counters have been introduced to measure the specific ionization, and combined with other devices, for instance Cherenkov counters, or magnet spectrometers, to determine energy or momentum. It is then not required that the particle be absorbed in the detector. The measured signals typically scale with Z^2, but for different devices exhibit characteristically different responses to energy. Cherenkov counters may use radiators that are solid, liquid, made of aerogel, or gaseous and hence, generate energy dependent signals over a wide range from less than 1 to at least 100 GeV amu^{-1}. Because of the required large size, most detectors for relativistic particles are flown on balloons, and a typical detector configuration is shown in Figure 9 [Lezniak 1978]. One detector system of relatively large area, developed by a Danish-French collaboration in the 1970's [Bouffard 1982] was designed for space observations, and was flown on the HEAO-3 satellite (1979–1981). This instrument permitted measurements of the elemental composition up to about 30 GeV amu^{-1}, and is shown in Figure 10.

[3] Note that E is the total kinetic energy of a cosmic-ray particle. For heavier nuclei of mass number A, quite often the unit E/A, the kinetic energy per nucleon, or the kinetic energy per amu, is used.

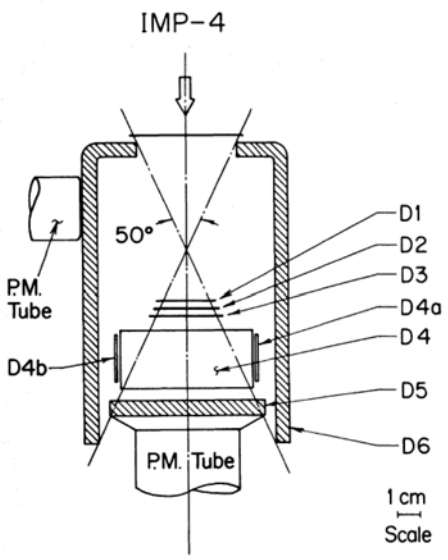

Fig. 8. Cross section of the University of Chicago IMP-4 telescope. D1, D2, and D3 are lithium-drifted silicon detectors; D4 is a CsI(Tl) crystal, viewed by Au-Si photodiodes. The telescope is surrounded by an anti-coincidence shield (shaded area) (figure from [Garcia-Munoz 1973]).

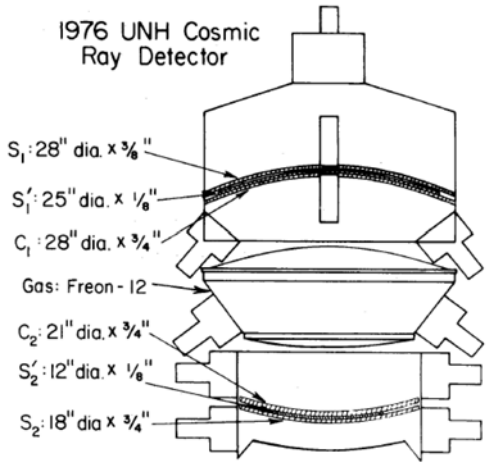

Fig. 9. Balloon-borne telescope of the University of New Hampshire. The detector contains plastic scintillators (S), Lucite Cherenkov counters (C), and a Freon-filled Gas Cherenkov counter, with diameters in inches as indicated (figure from Lezniak and Webber [Lezniak 1978]).

The cosmic rays constitute the only sample of matter from distant regions of the Galaxy that reaches the earth and is available for direct analysis. Thus, measurements on spacecraft and on balloons are aimed to provide sufficient detail to permit a quantitative comparison of the elemental abundances in the cosmic rays with the composition of other samples of matter, e.g. the composition of the solar system.

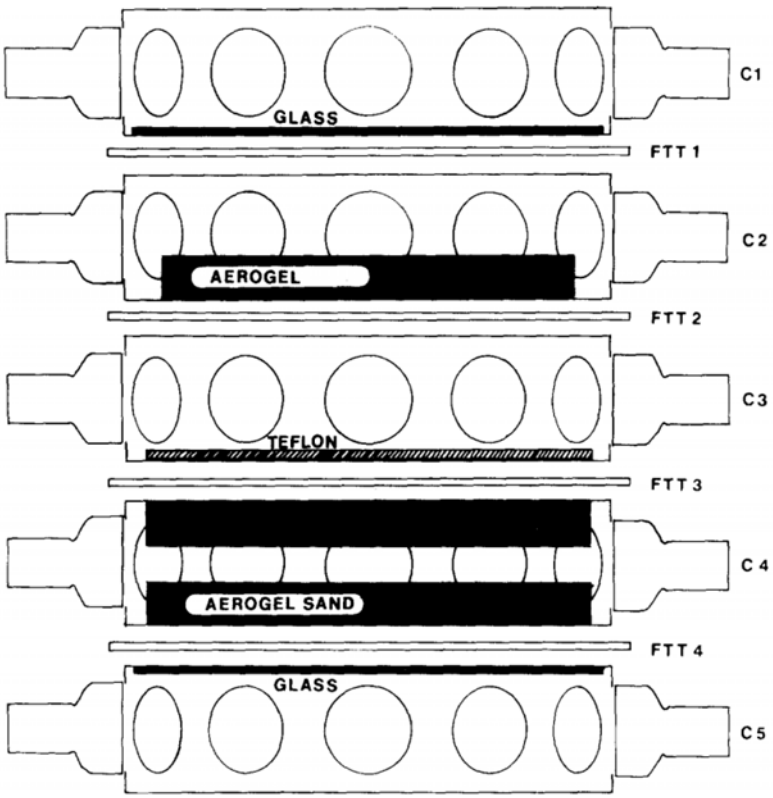

Fig. 10. Configuration of the Danish-French Cherenkov counter telescope on HEAO-3. The instrument has diameter of about 0.8 m (figure from [Bouffard 1982]).

Figure 11 shows a compilation of measurements, mostly made from the 1960's to the early 1980's [Simpson 1983] at energies up to a few GeV amu^{-1}. Plotted are the abundances of the elements He to Ni (relative to Si) in two energy regions. The low-energy data (70–280 MeV amu^{-1}) are measured on spacecraft [Garcia-Munoz 1979], while the results around 1–2 GeV amu^{-1} are from balloon flights [Dwyer 1981; Lezniak 1978; Webber 1982; Young 1981], and from observations on the HEAO-3 satellite [Binns 1981a; Engelmann 1981].

The abundances in Figure 11 are compared with the "Solar System" or "Universal" abundance distribution of the elements. This distribution is derived from the analysis of terrestrial, lunar, planetary, and meteoritic material, and from spectroscopic observations of the Sun, and of stars and the interstellar medium [Anders 1982].

The comparison reveals a number of highly interesting features. First, the relative abundances of the cosmic-ray components do not seem to be significantly altered by energy. Second, the overall appearance of the abundance distribution has similar features as the Solar system distribution, indicating that both samples of matter must have been generated by similar nucleosynthesis processes. However, there are also striking discrepancies: the light elements Li, Be, and B are dramatically more abundant in the cosmic rays than in the solar system. These elements cannot be final products of nucleosynthesis chains, and hence, cannot be part of the original cosmic-ray source material. Rather, they must be products of spallation reactions of the

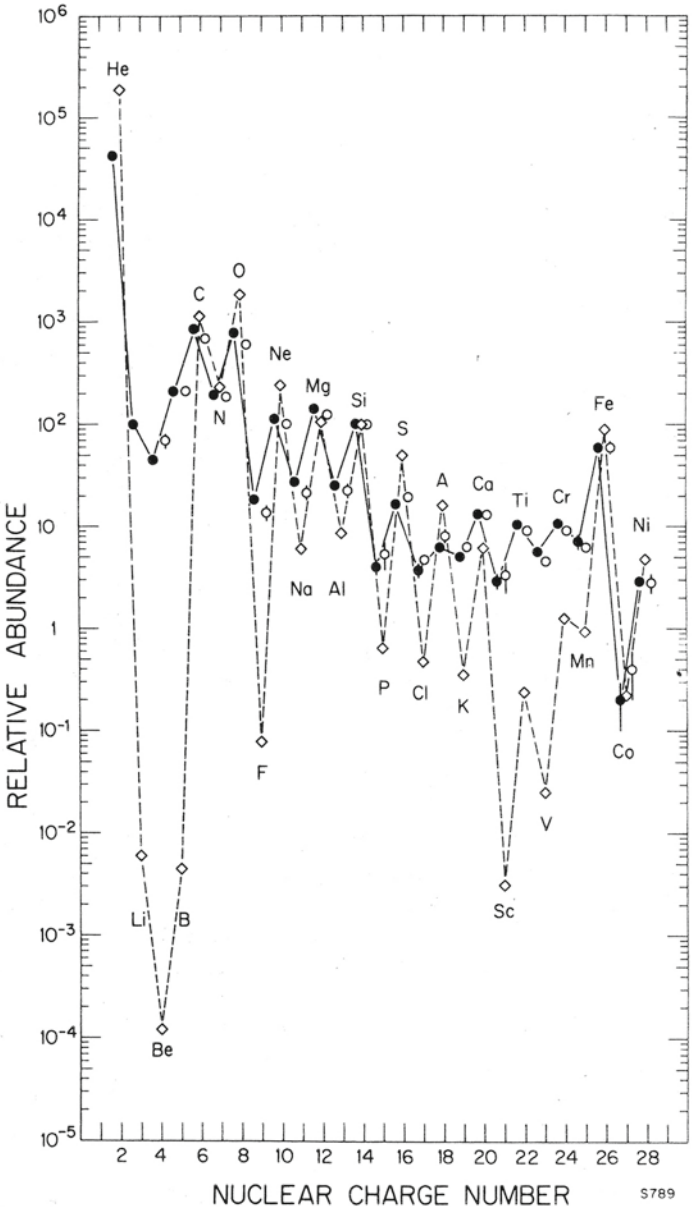

Fig. 11. Elemental abundances of cosmic rays from helium to nickel measured at Earth, compared to the solar system (or universal) abundance scale, all relative to silicon. Solid circles: low energy (70−280 MeV amu^{-1}); open circles: high energies (1000−2000 MeV amu^{-1}); open diamonds: solar system abundances (figure from [Simpson 1983]).

primary cosmic ray elements, in particular C and O, in the interstellar medium (ISM). A similar effect is seen for the elements Sc, V, and Mn which are mainly produced by spallation of Fe. Thus, one calls these elements "interstellar secondary cosmic rays" (not to be confused with atmospheric secondaries!), and their relative abundance has long been recognized to provide a measure for the amount of interstellar matter traversed on average by the primary parent nuclei: the interstellar path length (the

"propagation path length Λ") is derived to be about 10 g cm^{-2} at GeV-energies (see Sect. 4 and Fig. 37). It was later found that the path length decreases with energy (see Sect. 2.7.2). There are other and more subtle differences between the abundances of the primary nuclei in the cosmic rays and in the solar system. For instance, elements such as He, which have high first ionization potential (FIP), or high volatility, are less abundant in the cosmic rays than in the solar system (see Sect. 4). Understanding of this phenomenon is still subject of ongoing research.

2.5 Ultra-heavy cosmic rays

Elements heavier than iron must be produced in nucleosynthesis processes involving the capture of neutrons. Consequently, the relative abundances of these elements in the solar system are quite low. In the cosmic rays, such ultra-heavy nuclei have been discovered in the mid-1960's through the use of meteorites as space-borne detectors that have small size but exposure times of billions of years [Fleischer 1967a]. The observations were based on the detection of latent tracks in the meteoritic material that are caused by the large ionization energy-loss deposited by high-Z projectiles, and that could be made visible by chemical etching.

At the same time, observations on balloons and high-inclination satellites with large sheets of nuclear emulsions by the Bristol group [Fowler 1967], or with plastic track detectors by researchers at the General Electric Corporation (and colleagues at several institutions) [Fleischer 1967b; Price 1968], have identified the existence of ultra-heavy particles in the contemporary cosmic radiation.

These measurements motivated the construction of two dedicated satellite instruments in the late 1970's using electronic counter techniques, the British Ariel-6 [Fowler 1979], and the Heavy Nuclei Experiment led by M. Isreal on the NASA mission HEAO-3 [Binns 1981b]. The observational challenge for these projects was two-fold: first, the low particle intensities required large-area detectors, and second, exquisite charge resolution was needed. The HEAO instrument, consisted of a 2 m^2 stack of gas-ionization chambers, acrylic Cherenkov counters, and multi-wire ionization hodoscopes. The placement of this instrument in the HEAO-3 payload is illustrated in Figure 12. The elemental composition of cosmic rays, including results from these measurements [Binns 1989], is summarized in Figure 13 [Wiedenbeck 2007].

As Figure 13 illustrates, the abundances of the cosmic-ray elements above iron drop off dramatically with increasing charge number Z, showing the same behavior as the universal elemental abundances (here called solar system abundances [Lodders 2003]). Identification of individual elements becomes increasingly difficult, and above $Z = 60$, only groups of elements have been identified.

The distribution of the heaviest elements is thought to carry very specific information about the history and nucleosynthesis of cosmic-ray material. Hence, improved resolution in charge and better statistical accuracy are desired. Excellent charge resolution has been demonstrated with new passive detectors using sheets of plastic and glass materials that are chemically etched after exposure. An array of such detectors (called TREK) was exposed on the Russian MIR space station between 1991 and 1994 [Weaver 2002]. TREK indeed has resolved the elements in the region $Z = 72$ to 82, i.e. around platinum and lead, which are key indicators for the contributions of "rapid" or "slow" neutron capture processes during nucleo-synthesis.

Recent measurements with new active detectors have been made on long-duration balloons with the TIGER instrument [Link 2001] which combines large-area aerogel and acrylic Cherenkov counters with a scintillating fiber hodoscope that records the particle trajectories (see Fig. 14). An upgraded version ("Super-TIGER") is currently in preparation.

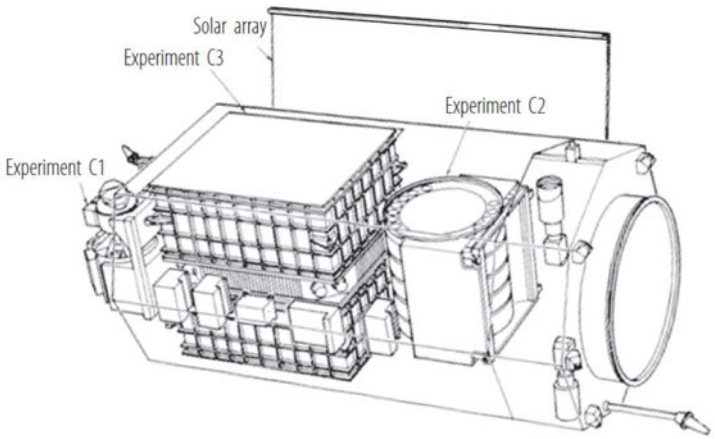

Fig. 12. HEAO-was the largest free-flying satellite for early cosmic-ray observations, flown 1979–1981; Shown here is drawing of the payload bay with the Heavy Nuclei Experiment (C3) and the Danish-French detector (C2, see Sect. 2.7.2) (figure from [Bouffard 1982]).

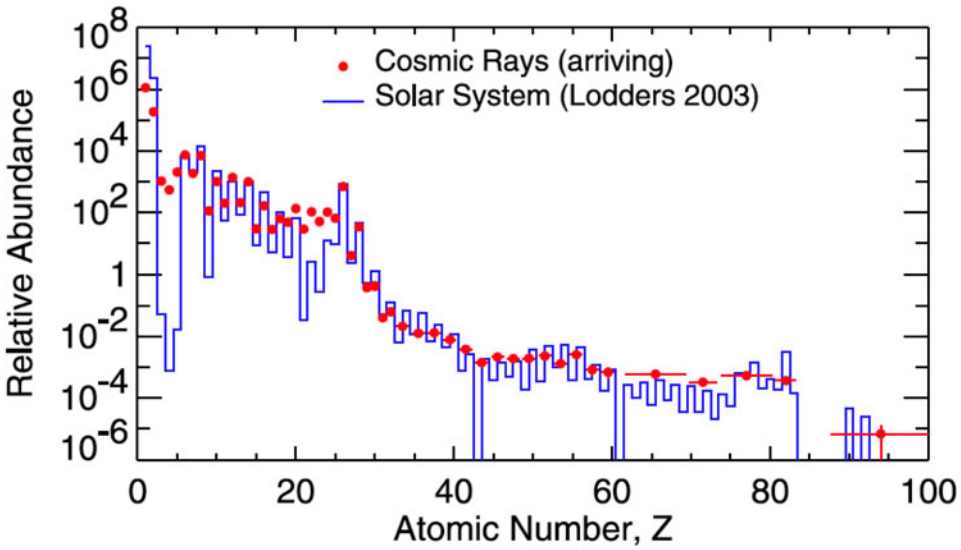

Fig. 13. Compilation of elemental abundances in the arriving cosmic rays (filled circles) compared with those found in solar-system material (histogram). Cosmic-ray data correspond to energies $\lesssim$1 GeV amu^{-1}. Points for ultraheavy cosmic rays [Binns 1989] are shown with abundances averaged over adjacent odd-even element pairs ($33 \leqslant Z \leqslant 60$) or over larger groups ($Z \geqslant 60$) (figure from [Wiedenbeck 2007]).

2.6 Isotopic abundances

A cosmic-ray nucleus is characterized completely if, in addition to its energy or momentum, not only the nuclear charge Z, but also the mass number A is measured. It had long been realized that the isotopic distribution may carry characteristic imprints of nucleosynthesis chains, and that radio-active isotopes may serve as cosmic-ray clocks. However, the precision required for isotopic composition measurements presents a formidable challenge to the observer. The most successful measurements

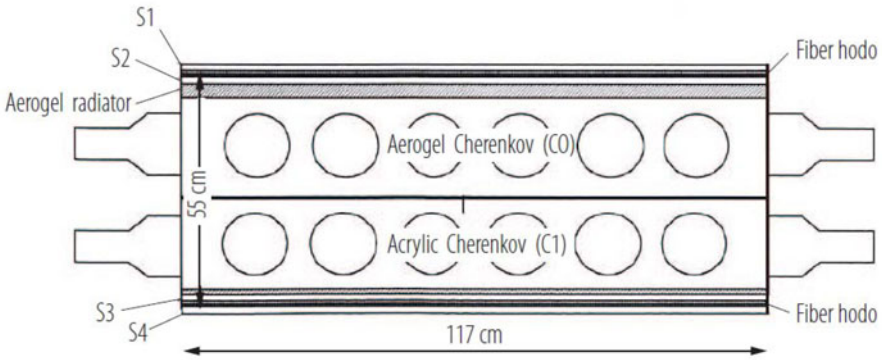

Fig. 14. Cross section of the TIGER instrument for ultra-heavy cosmic rays (from [Link 2001]).

rely on refining the signal resolution obtainable with the dE/dx vs. E method (see Sect. 2.4) with solid-state detectors for particles of sufficiently low energy to be absorbed in the detector completely. Details of this technique can be found, for example, in the description by Stone et al. of the detectors flown on the Advanced Composition Explorer (ACE) [Stone 1998a; 1998b].

Intrinsic limitations to the precision of an instrument such as that shown in Figure 8 come from signal fluctuations due to variations in the particle's path length through the detector for different angles of incidence. An improvement has been achieved through an apparently simple trick, the use of curved detectors as shown in Figure 15 for instruments flown on spacecraft IMP-7 and IMP-8 (launched in the early 1970's; IMP-8 remained active until 2006): the geometric path length fluctuations for particles entering the detector from different directions are reduced. Note that curved detectors were also used by Webber and collaborators in balloon-borne observations, as shown, for instance in Figure 9.

Indeed, the IMP instruments did achieve isotopic separation for elements at relatively low Z [Garcia-Munoz 1975a]. One of the most interesting results from these observations was the discovery that the relative abundance of the radio-active ^{10}Be isotope (β^+ decay, half life 1.5×10^6 years) is surprisingly low [Garcia-Munoz 1975b]. This isotope must have largely decayed during the "containment time τ" of the cosmic rays in the Galaxy. A value of τ of about 10^7 years could be derived from the measurement, much larger than expected, and could only be consistent with the measurement of the propagation path length (see Sect. 2.4) if the containment volume of the cosmic rays includes a halo surrounding the Galactic disk.

Solid-state detector telescopes with curved Si-detectors were also developed by a collaboration led by Caltech and NASA GSFC [Stone 1977] for the Voyager 1 and 2 deep-space missions launched in the late 1970s. These instruments (shown in Fig. 16) were active for two decades and provided isotope measurements (e.g. [Lukasiak 1994a; 1994b; 1994c; Lukasiak 1997], in addition to a wealth of information on particle astrophysics in the Solar System.

Later generations of instruments incorporated active particle hodoscopes in order to determine the trajectory of each cosmic-ray nucleus through the instrument. The ^{10}Be measurement just mentioned was confirmed by the Berkeley group [Wiedenbeck 1980] with improved precision with a detector on the ISEE mission, using drift chambers for trajectory determination. An instrument on the Ulysses mission (launched 1986, and exploring the Solar System above and below the ecliptic plane until 2009), incorporated silicon-strip detectors [Simpson 1992]. For the currently largest and most advanced detector system, the CRIS instrument on the advanced composition explorer

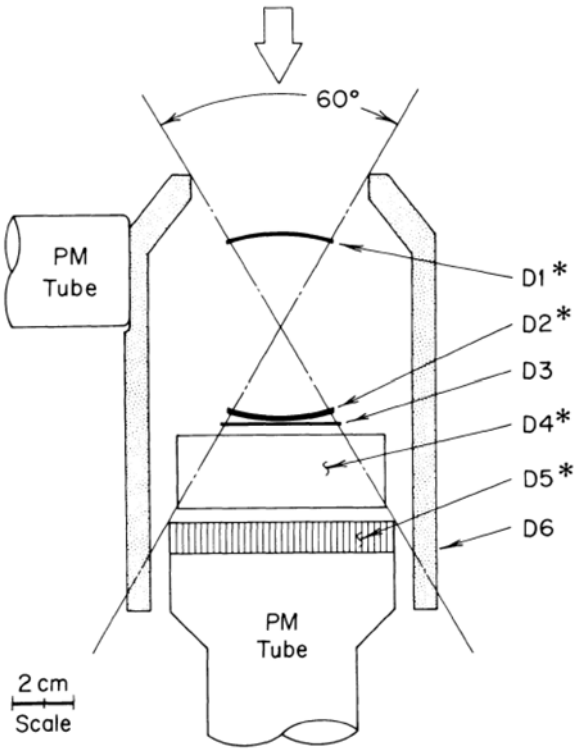

Fig. 15. Cross section of the University of Chicago detectors flown on IMP-7 and IMP-8. Note that the detector arrangement is similar to that of the dE/dx vs. E system of Figure 8. However, two of the the three Li-drifted Si-detectors are curved in order to minimize pathlength variations of traversing particles (figure from [Garcia-Munoz 1975a]).

(ACE, launched in 1997), stacks of silicon-detectors are combined with a hodoscope of scintillating fibers [Stone 1998a].

Figure 17 summarizes the isotopic composition data that are currently available from the CRIS-ACE detector. The mass resolution is impressive, and the data contain an amount of information which to discuss is beyond the scope of this review. Overall, it appears that the isotopic composition of the cosmic rays is surprisingly similar to the universal abundance scale, with a few exceptions such as an over-abundance of the ^{22}Ne isotope (see Sect. 4 for further detail). The earlier ^{10}Be results have been confirmed by CRIS with higher accuracy, and consistent values of the containment time τ have also be obtained with other long-lived "clock isotopes", ^{26}Al, ^{36}Cl, and ^{54}Mn [Yanasak 2001].

Another example of interesting timing information is the ^{59}Ni isotope. This nucleus should be included in the material ejected from SN explosions. However, it is not found in the cosmic rays (see Fig. 18). ^{59}Ni decays by electron capture into ^{59}Co at a half life of 7.6×10^4 years if electrons are present. ^{59}Co is observed in the cosmic rays. Thus, the ^{59}Ni nucleus must have "lived" in a low-energy plasma containing slow electrons and cannot have been accelerated to relativistic energy for about 10^5 years after the SN explosion [Wiedenbeck 1999]. This conclusion contributes to other evidence that the seed material of cosmic rays is old interstellar gas rather than the fresh SN ejecta.

All observations of the isotopic composition that rely on the dE versus E technique are necessarily restricted to relatively low cosmic-ray energies, where the particles can

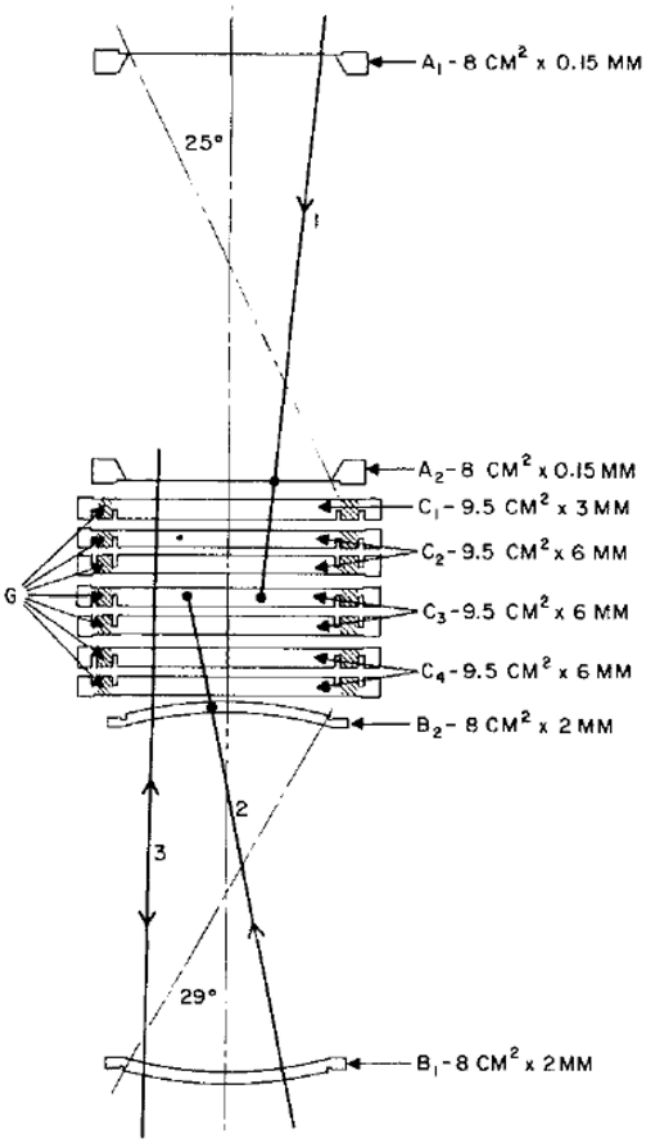

Fig. 16. Cosmic-ray telescope for the Voyager and missions. Notice that the telescope is double-ended, accepting particles arriving from two opposite directions (figure from Stone [1977]).

be slowed down and absorbed within the detector. It is desirable to extend the measurements into the highly relativistic region. For example, the abundance of clock elements such as ^{10}Be for varying relativistic time dilatations should reveal the distribution of containment times of cosmic rays in the Galaxy. Attempts have been made to use the classic mass-spectrometer technique for such measurements: particles are deflected in a magnetic field (preferably from a superconducting magnet on balloon or in space) to measure their momentum, and their velocity may be determined with time-of-flight techniques (still limited to relatively low energies), or with Cherenkov counters. However, it is extremely challenging to reduce the statistical and systematic

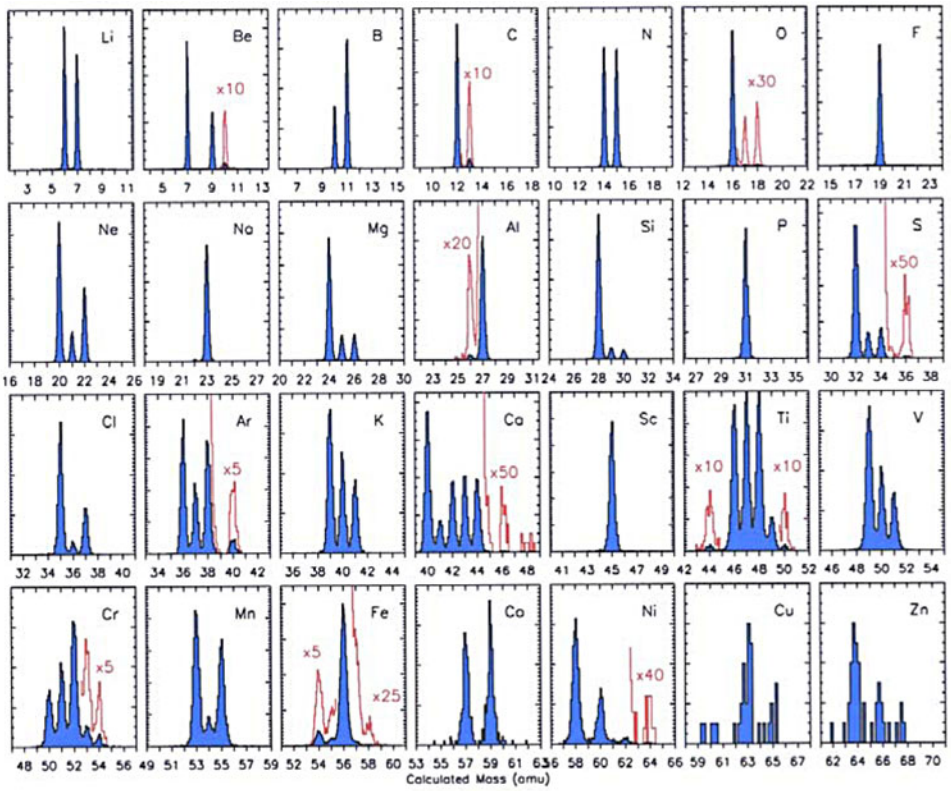

Fig. 17. Relative isotopic abundances of the elements from Li to Zn. Measurements with the CRIS instrument on the ACE mission. Unfilled histograms (in red) indicate amplified vertical scales (figure from ACE science center web site).

measurement uncertainties in such instruments to a level commensurate with the required mass resolution. Therefore, successful measurements have been restricted to the isotopes of the light elements up to to boron, and to energies not exceeding a few GeV amu^{-1}. For instance the superconducting magnet spectrometers SMILI [Ahlen 2000; Ficenec 1993] and IMAX [Mitchell 1993] have reported results on the light isotopes. These instruments were developed by collaborations of several institutions in the US and in Europe. Eventually, a collaboration led by Streitmatter of NASA-GSFC, and including the California Institute of Technology and the University of Siegen (Germany), constructed a larger balloon telescope called ISOMAX which was flown in 1998 (but unfortunately, was destroyed in a subsequent flight attempt in 2000). ISOMAX provided the first data on the relative abundances of the beryllium isotopes around 2 GeV amu^{-1} [Hams 2004].

Such spectrometers are also used for the identification of the rare anti-particles (positrons and anti-protons) in the cosmic rays, and additional comments about the magnet spectrometer technique will be given in Section 3.1.

2.7 Energy spectra

The shape of the energy spectrum of a cosmic-ray component carries the imprint of the Galactic accelerator for this component. However, the spectrum may also be affected by energy-dependent effects during propagation through the ISM. For energies

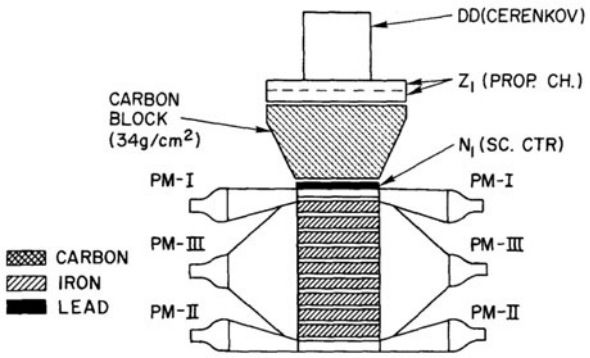

Fig. 18. Schematic cross section of the calorimeters (SEZ-14) flown on the PROTON missions 1, 2, and 3 (figure from [Grigorov 1971c]).

less than about 10 GeV amu^{-1}, solar modulation changes the energy spectrum of the particles arriving at earth, and only at higher energies can the measurements reveal the spectrum of ambient Galactic particles directly. As the energy increases, such measurements become increasingly difficult for two reasons: first, the intensities decrease rapidly and second, there are few techniques for energy measurements of highly relativistic particles that are practical for balloon or space applications. The observation of the more abundant species hydrogen and helium on the one hand, and of the heavier nuclei on the other, must meet different experimental challenges, for instance large signal fluctuations for the charge measurement of H and He, but very low intensities for the heavier nuclei.

2.7.1 Protons and helium

Ionization calorimeters that are several interaction lengths thick can provide an energy measurement at moderate resolution as they absorb a good fraction of the energy of the nuclear cascade generated by a primary particle. However, the absorber must be very deep in mass, and in order to keep the instrument weight manageable, the calorimeter is limited in area, and thus, is better suited for measurements of the more abundant elements, hydrogen and helium than for the heavier nuclei. Such calorimeters have been proposed by Grigorov and collaborators at Moscow State University since the 1950s [Grigorov 1966], and have been used in a series of satellite observations with the Soviet PROTON Spacecraft (PROTON 1-4) in the 1960s [Grigorov 1970]. Figure 18 shows schematically the design of one of these instruments. The PROTON spacecraft were able to carry very massive instruments; the calorimeter on PROTON-4 is said to have had a mass of 12.5 tons [Panasyuk 2011] which probably would make it the heaviest cosmic-ray detector ever carried above the atmosphere.

The Proton missions determined the all-particle energy spectrum of cosmic rays over a wide energy range, from about 10^{11} to 10^{15} eV [Grigorov 1971a]. The results of these investigations are included in the all-particle spectrum shown in Figure 19. However, the measurement of the energy spectra of individual elements turned out to be more difficult. The PROTON results indicated a spectrum for hydrogen that became steeper above 10^{12} eV than that of helium, and of groups of heavier elements [Grigorov 1971b; 1971c].

One of the subtle difficulties with calorimeters comes from the fact that the nuclear cascade entails a huge number of secondary particles (mostly pions, muons, electrons and photons). Some of these secondaries may scatter upwards and make it difficult to unambiguously identify the incident primary particle, in particular if this particle

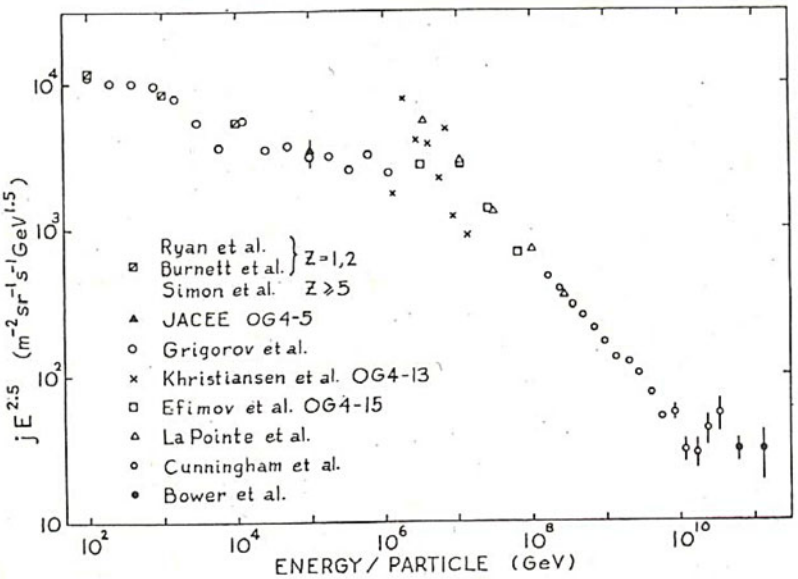

Fig. 19. The all-particle energy spectrum of cosmic rays, multiplied with $E^{2.5}$, as it was known in the early 1980s [Linsley 1983]. The "knee" above 10^{15} eV is noticeable, and all data above that energy are from indirect air-shower observations. Most of the data below the knee result from the PROTON 1-missions [Grigorov 1971a].

is singly charged (i.e. a proton). Hence the detection efficiency at the higher energies may be compromised [Ellsworth 1977]. Attempts to remedy the back-scatter problem in later and in current calorimeters (including the currently used short calorimeters, see below) are made through the use of spatially segmented counters. This approach was implemented, for instance, by the Moscow group in the SOKOL missions in the 1980s, and the anomalous steepening of the proton spectrum was then not confirmed [Ivanenko 1988].

Total-absorption calorimetry with a four interaction lengths deep detector was also attempted on balloon with a NASA balloon project in the 1970s that is shown in Figure 20 [Ryan 1972]. However, for weight reasons, alternate approaches for balloon payloads were later developed. These would either be non-calorimetric detectors optimized for protons and helium, and usually restricted to a limited range of energies, or so-called short calorimeters.

Non-calorimetric measurements on balloon were made with several superconducting magnet spectrometers from the 1970s to the present time [Boezio 2000; Haino 2004; Mitchell 1996; Seo 1991; Smith 1972], and with a ring-imaging gas Cherenkov counter in the 1990s [Buckley 1994; Diehl 2003]. The AMS collaboration deployed a magnet spectrometer (with permanent magnets) for exposure on the Space Shuttle in 1998 [Aguilar 2002], and on the Space Station in 2011. The international PAMELA space mission with a permanent magnet spectrometer (see Fig. 31) was launched in 2006 [Adriani 2011a]. For additional comments on magnet spectrometers, see Section 3.1.

Several groups developed the concept of short calorimeters and implemented it on long-duration balloons from the 1980s until the present time. In such detectors, a primary cosmic-ray nucleus undergoes a hadronic interaction, but only the onset of the nuclear cascade generated by pions, electrons and photons from the first interaction, is detected in an electro-magnetic shower counter. Instruments that used this approach with passive emulsion-stack detectors are the American-Japanese project JACEE in

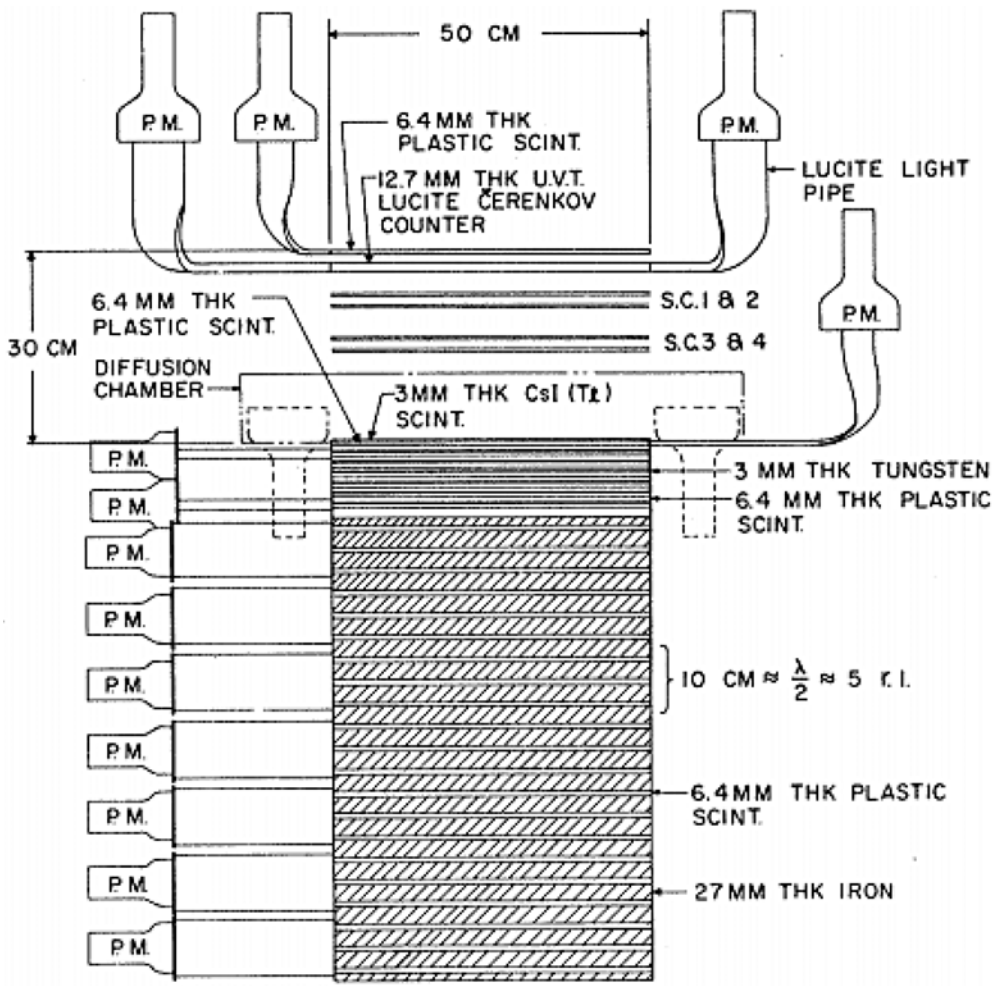

Fig. 20. Balloon-borne ionization spectrometer. SC_1, SC_2, SC_3, and SC_4 are spark chambers to determine the trajectory of the incident particle and to help in rejecting background events. The calorimeter consists of sandwich of tungsten or steel layers, interleaved with plastic scintillators (figure from [Ryan 1972]).

the 1980s–1990s [Asakimori 1998; Burnett 1986], and the Russian-Japanese RUNJOB in the 1990s [Apanasenko 2001]. Active electronic detector systems are employed by the international collaborations ATIC (with collaborators in USA, Russia, S. Korea, and China) and CREAM (USA, Russia, and S. Korea) in the 2000s [Ahn 2007; Guzik 2004]. As an example for such instruments, ATIC is shown in Figure 21. These instruments led to measurements of protons and helium, and of the spectra of heavier nuclei, although for the initial observations (e.g. JACEE), the charge resolution was limited and allowed only the identification of groups of charges.

Most results of these measurements indicated differential energy spectra for both species, p and He, over the range 10 to several 100 GeV amu^{-1}, in the form of power laws in energy $E^{-\alpha}$ with the same power law exponent $\alpha \approx 2.75 \pm 0.1$. This result might be expected if both species are accelerated by the same mechanism. However, PAMELA reported that the spectrum of protons is slightly steeper than that of helium at these energies [Adriani 2011b]. The PAMELA result is shown in Figure 22. A

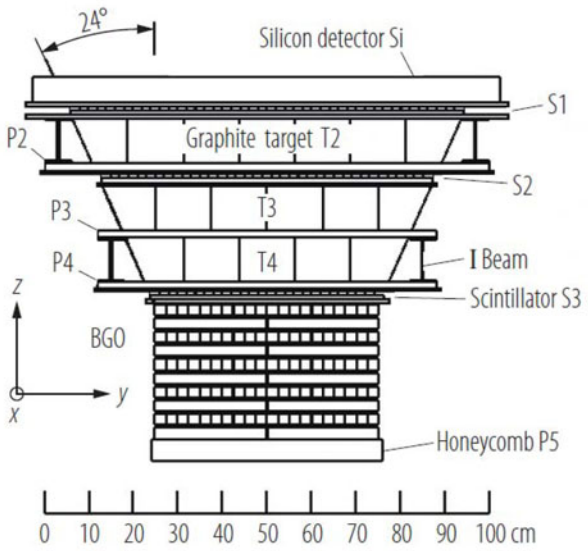

Fig. 21. Cross section of the ATIC configuration. Cosmic-ray nuclei may interact in the graphite target, and the BGO calorimeter analyzes the electron-photon cascade from this interaction (figure courtesy of G. Guzik, Louisiana State University).

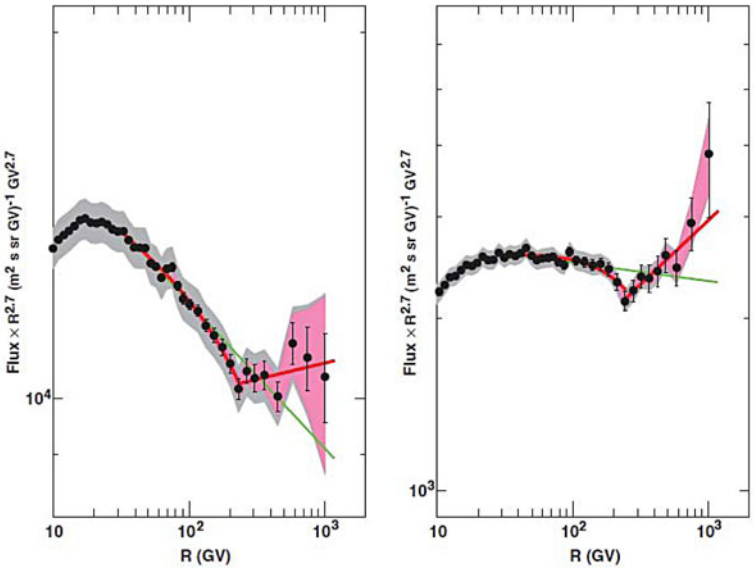

Fig. 22. Proton (left) and Helium (right) rigidity spectra multiplied with $R^{2.7}$ in the range 10 GV to 1.2 TV, measured by PAMELA. The shaded areas represent the estimated systematic uncertainties (figure from [Adriani 2011b]).

similar effect was reported by the CREAM group for the highest energies (10^3 to 10^5 GeV amu^{-1}) that could be covered thus far: As shown in Figure 23, there may be a slight softening of the spectra of both protons and helium above 100 GeV amu^{-1} which is more pronounced for helium than for protons [Yoon 2011]. Unless these subtle differences in spectral shape are caused by unknown systematic uncertainties, they are difficult to explain with standard cosmic-ray models.

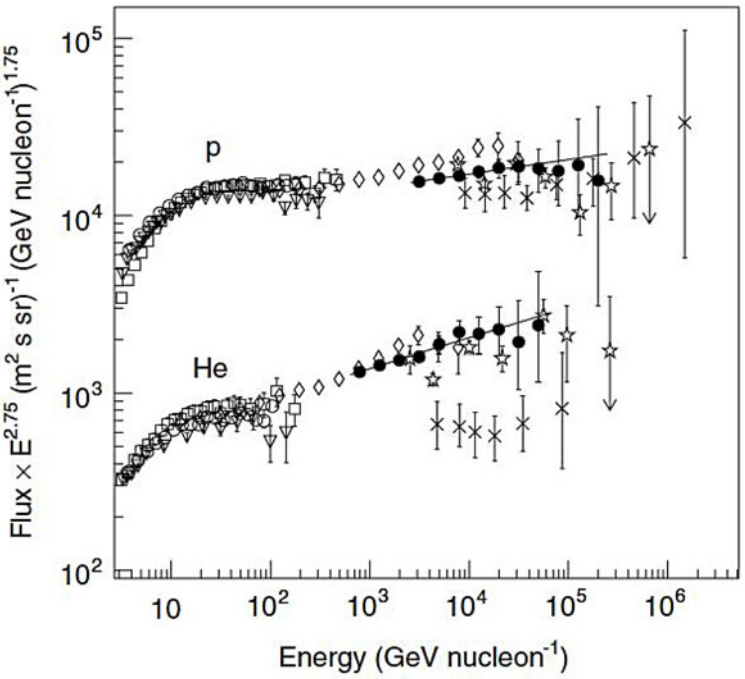

Fig. 23. Energy spectra (multiplied with $E^{2.75}$) for protons and helium nuclei. (Compilation of data by [Yoon 2011]).

2.7.2 The heavier nuclei

The low intensities of nuclei heavier than helium require very large detector systems and/or extended observation times if measurements at high energies are to be made. On the other hand, signals typically increase with Z^2, and therefore, relative signal fluctuations decrease as $1/Z$. Hence, rather weak effects such as the relativistic rise of ionization loss in gases, or gas Cherenkov counter signals, have been utilized for energy measurements. At the highest energies, around and above 1000 GeV amu^{-1}, the emission of X-ray transition radiation has been successfully used to determine the cosmic-ray energy [Müller 2004]. This technique was first utilized in the Cosmic-Ray Nuclei Detector (CRN) flown on the Space Shuttle in 1985 [L'Heureux 1990; Müller 1991] and subsequently in the TRACER detector on long duration balloon flights in the 2000's [Ave 2011]. These instruments are shown in Figure 24.

The first measurements of the elemental abundances of the heavier elements reaching the 100 GeV amu^{-1} range were made on balloons in the early 1970's, and immediately led to a surprise: it was found that the relative abundances of the secondary nuclei, such as Li, Be, and B, decreased fairly rapidly as the energy increased. This discovery was made with a gas Cherenkov counter telescope of the Chicago group [Juliusson 1972], shown in Figure 25, and with the first balloon-borne superconducting magnet spectrometer developed by the Berkeley group [Smith 1973]. This unexpected effect was confirmed with high statistical accuracy with the Danish-French instrument that flew on HEAO-3 [Engelmann 1990], see Figure 10. Later observations with the CRN instrument in 1985 [Swordy 1990] and with long-duration balloon flights of CREAM [Ahn 2008], ATIC, [Panov 2007] and TRACER [Obermeier 2011] have extended the measurements of the secondary/primary abundance ratio to

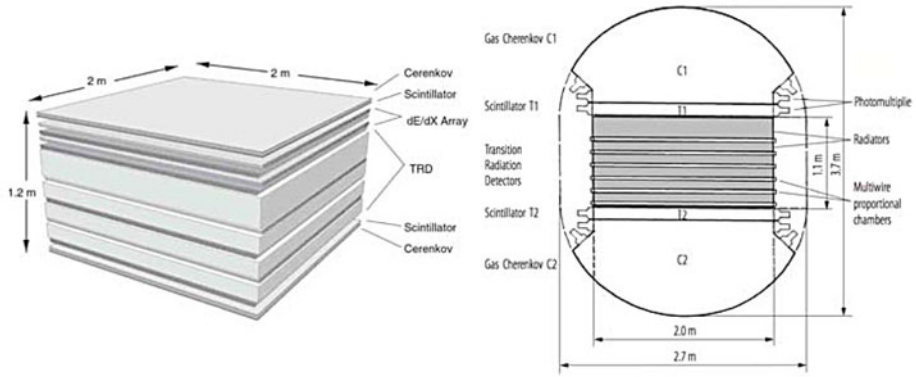

Fig. 24. The TRACER cosmic-ray detector (left) consists of a large-area plane sandwich of plastic Cherenkov and scintillation detectors, and proportional tubes to detect particle ionization loss (dE/dx) and transition radiation. The predecessor for TRACER was the CRN instrument (right) which combined a transition radiation detector employing multi-wire proportional chambers with two gas Cherenkov/scintillator combinations (figures from [L'Heureux 1990; Obermeier 2011]).

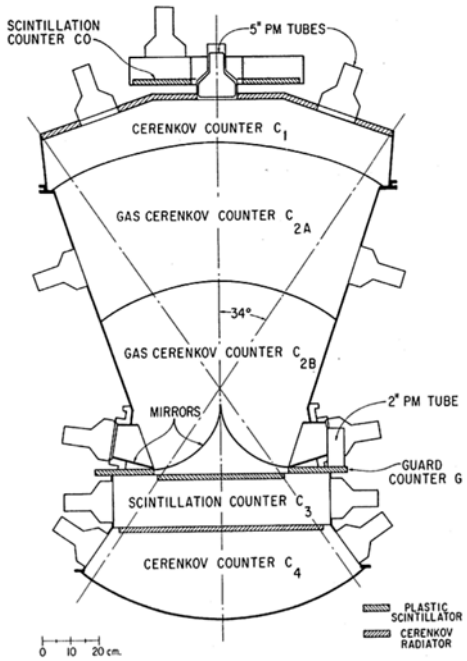

Fig. 25. Gas-Cherenkov detector system for balloon flights in the 1970's (figure from [Juliusson 1972]).

energies around 1000 GeV amu^{-1}. A compilation of data on the abundance of boron relative to carbon (the "B/C ratio") is shown in Figure 26.

The decrease of the relative abundance of secondary particles implies that the cosmic rays escape faster from the Galaxy and traverse less and less interstellar matter as the energy increases (from around 10 g cm^{-2} at 10 GeV amu^{-1} to less than 1 g cm^{-2} at 1000 GeV amu^{-1}; see Fig. 37). The details of propagation through the Galaxy that

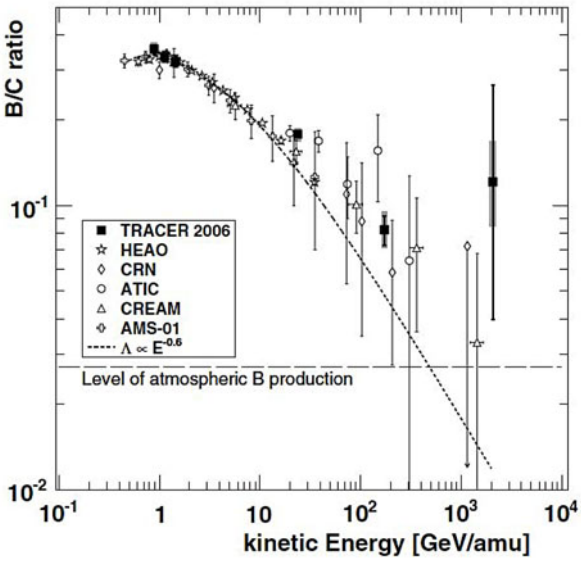

Fig. 26. The abundance ratio of Boron (secondary) to Carbon (primary) vs. energy. (Compilation of data: [Obermeier 2011], and references therein).

lead to this effect are still not well understood. However, the equilibrium between production and escape then requires that the energy spectrum of the cosmic rays at the acceleration sites (the sources) is harder than that observed near earth. This fact, which will be further discussed in Section 4, strongly supports an acceleration mechanism that was proposed in the late 1970s: acceleration in the shock fronts moving away from supernova explosions [Axford 1977; Bell 1978; Blandford 1978]. This process predicts hard source energy spectra, with a spectral index that may be as low as 2.0 for strong shocks. The shock mechanism is a Fermi process in the first order of u/c (where u is the shock speed) and hence, quite efficient. It has now become the favored theory for cosmic-ray acceleration up to the "knee" of the overall energy spectrum (around 3×10^{15} eV per particle). Direct observational evidence from the detection of high-energy γ-rays from supernova remnants, is however still controversial.

It is now a long-standing goal to measure the individual energy spectra of all primary cosmic-ray components up to energies close to the "knee", the overall change in the slope of the all-particle energy spectrum observed in air-shower measurements above 10^{15} eV. It has been predicted that the shock-acceleration mechanism becomes inefficient at these energies [Lagage 1983] and that, consequently, the cosmic-ray composition undergoes characteristic changes. No telling changes have been found in observations made with the instruments mentioned above: CRN on the space shuttle in 1985 [Müller 1991], TRACER in the 2000's [Ave 2008; Obermeier 2011], and the short calorimeters, RUNJOB [Apanasenko 2001], ATIC [Guzik 2004], and CREAM [Ahn 2008; Yoon 2011] in the 2000's. It appears that all primary cosmic-ray nuclei are characterized by a very similar form of their energy spectrum, in first order a power law with index $\alpha = 2.65 \pm 0.05$ in the 10–1000 GeV amu^{-1} region. More recently, the CREAM collaboration has reported a slight hardening of the energy spectra above 200 GeV per amu [Ahn 2010], but this effect seems to be at the limit of the statistical uncertainty of the data. Figure 27 shows a compilation of differential energy spectra, mostly from these measurements, as given in the Review of Particle Physics [Amsler

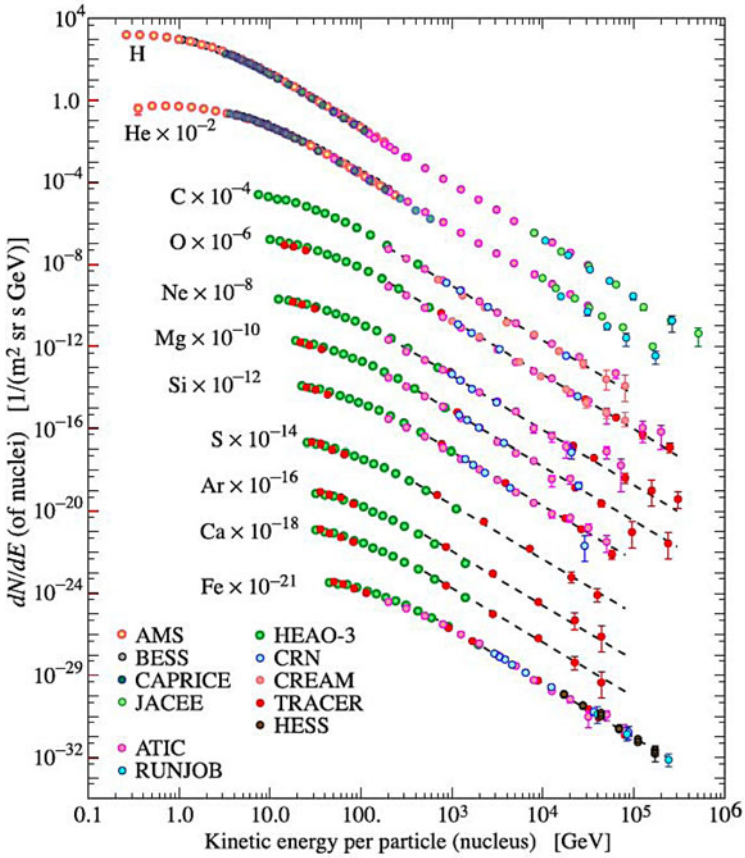

Fig. 27. Compilation of the energy spectra of the individual cosmic-ray elements from protons to iron (figure from [Amsler 2008]).

2008]. It should be noted that this figure uses a highly compressed scale. Therefore the hardening of the spectra just mentioned, and the differences in the spectral shapes for protons and helium discussed in Section 2.7.1, are not easily discernable in Figure 27. In Figure 28, we use the energy spectrum of iron nuclei to illustrate the variety of techniques that have been applied for measurements in different energy regions (from [Ave 2011]).

3 Observations of electrons, positrons, and anti-protons

3.1 Electrons and positrons

Results from two independent balloon observations, announced in 1961 by observers in Minnesota and in Chicago, respectively [Earl 1961; Meyer 1961], demonstrated that the primary cosmic rays also contain electrons, albeit at an intensity at energies around 1 GeV that is lower by about two orders of magnitude than the intensity of protons. The characteristic observational features utilized in these and in all subsequent electron measurements are the electromagnetic showers which develop rapidly in high-Z absorber materials such as lead or tungsten. However, the much larger intensity of protons generates a background of showers induced by protons or secondary

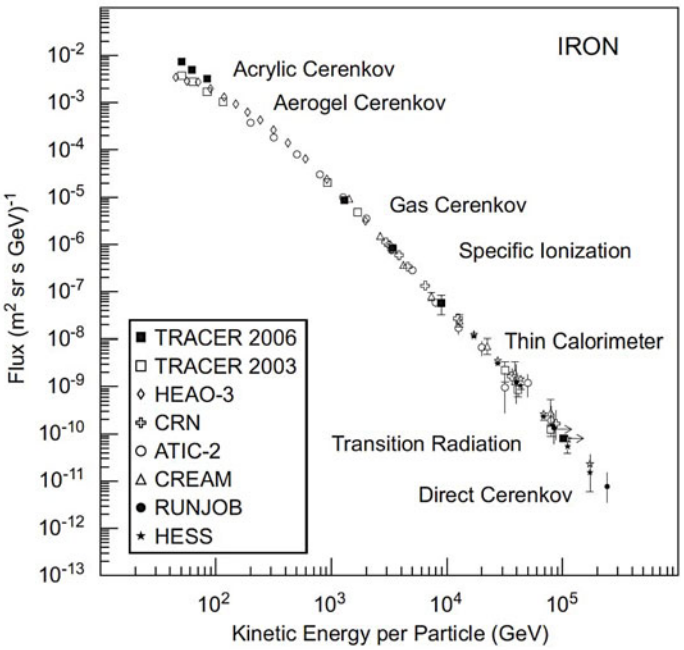

Fig. 28. Energy spectrum of iron nuclei, indicating the measurement techniques used for different portions of the energy range. Note that the data at the highest energy are from ground-based observations of the direct Cherenkov light emitted before the iron nucleus interacts in the atmosphere. These observations were made with the HESS Cherenkov telescope array (figure from [Ave 2011]).

pions which to identify and reject remains the major (and not always successfully mastered) experimental challenge to electron and positron observations until the present time.

From the outset, there was great interest in studies of electrons because their intensities may be strongly affected by electro-magnetic interactions in the ISM, in particular synchrotron radiation in the galactic magnetic fields, and inverse Compton scattering with photons of the cosmic microwave background. Neither process affects the nuclear cosmic rays because of their much larger mass, but both cause electrons to lose energy at a rate that increases with the square of the electron energy. Thus, assuming that electrons are accelerated in sources together with the nuclear cosmic rays at comparable energies, the imprint of these processes should be seen in the observed energy spectrum. Consequently, in the 1970's and 1980's, many groups attempted measurements over a large energy range, using either electronic calorimeters [Hartmann 1977; Prince 1979; Silverberg 1973; 1976; Tang 1984] or passive emulsion stacks [Anand 1975; Nishimura 1980]. Different methods were employed to identify proton background, including calorimeters of great depth, gas-Cherenkov counters, time-of-flight techniques, transition radiation detectors, and visual inspection of emulsion tracks.

The shape and absolute normalization of the energy spectrum of electrons initially remained controversial, but in the late 1970's, it became clear that the electron intensity between 10 and several 100 GeV dropped with energy significantly faster than the intensity of protons and nuclei.

Improving and extending these measurements with good accuracy, in particular in the high-energy region above 100 GeV, has remained a challenging task until the

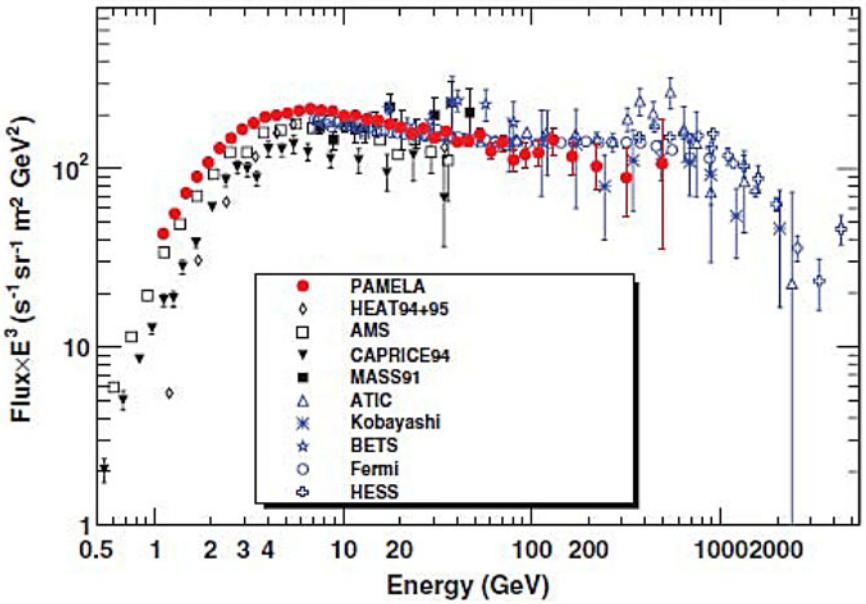

Fig. 29. The differential energy spectrum of electrons (multiplied with E^3). Note that the data points indicated in blue refer to the total electron intensity ($e^+ + e^-$), while the remainder are measurements of e^-. (Compilation of data by [Adriani 2011a], see references therein)

present time. In Figure 29 we summarize the current knowledge of the electron energy spectrum, based on measurements since the 1980s. Note that the plotted intensities are multiplied with E^3. These data come from balloon-borne observations with shower counters [Chang 2008; Kobayashi 1999; Torii 2001], some combined with magnet spectrometers [Boezio 2000; DuVernois 2001; Grimani 2002], and from three instruments on spacecraft, the magnet spectrometers AMS-01 [Alcaraz 2000], PAMELA [Adriani 2011a], and the Fermi LAT gamma-ray detector [Ackermann 2010]. A data set derived from ground observations with the HESS TeV gamma-ray telescope is also shown [Aharonian 2008]. There are still considerable uncertainties in the measurements, and data sets of different observers do not always agree within quoted error bars. At low energies, below 10 GeV, this may be due to different solar modulation levels of individual observations, but at higher energies, there are obvious systematic uncertainties.

Nevertheless, the energy spectrum of electrons between 10 and 1000 GeV decreases approximately as a power law in energy with spectral index 3.1 ± 0.1. The spectrum falls more steeply than that of cosmic-ray nuclei (see Sect. 2.7) as is expected as a consequence of radiative energy losses in the galaxy. There may be some deviations from the power-law character: the ATIC group [Chang 2008] has reported a broad peak around 600 GeV. Particularly interesting is the possibility of a spectral cut-off in the TeV region as hinted by the HESS results. This cutoff, if it indeed exists at these energies, could signify that TeV electrons can no longer travel the distance from their sources to the solar system. Such a cutoff would be quite analogous to the "Greisen, Zatsepin, Kuzmin (GZK) Cutoff" of extragalactic protons at the highest energies (10^{19}–10^{20} eV).

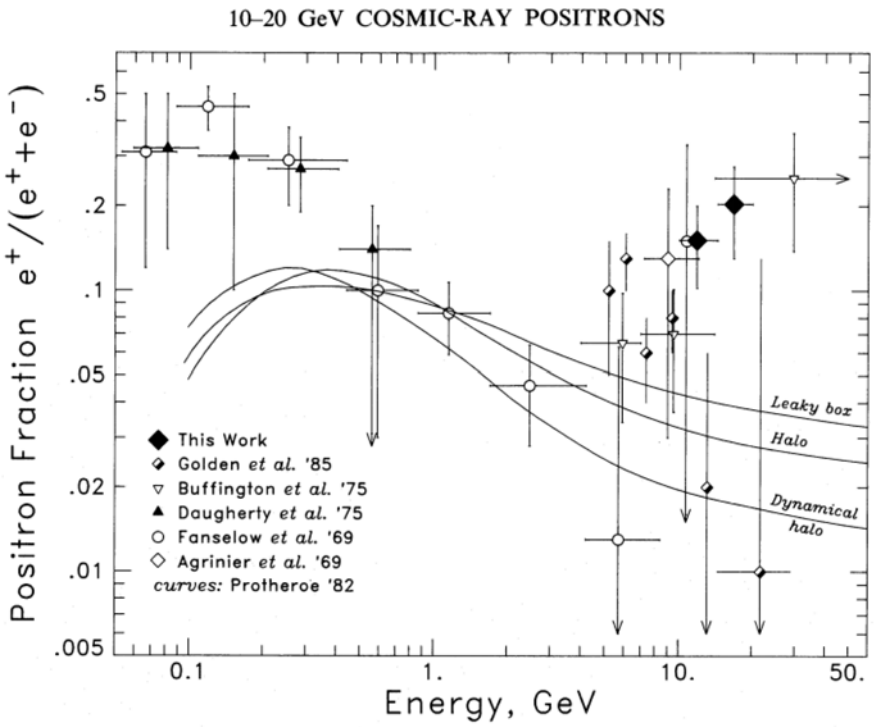

Fig. 30. Early measurements of the relative intensity of positrons. The curves refer to predictions for purely secondary production according to several models. (figure from [Müller 1987], see references therein).

Already the initial electron observations in the early 1960s raised the question whether these particles are indeed accelerated in primary cosmic-ray sources, or whether they are just of interstellar secondary origin, generated by pions from nuclear interactions of protons via the $\pi \rightarrow \mu \rightarrow e$ decay chain. In the first case, the electrons would be expected to be essentially all be negative, i.e. of "ordinary matter" origin, while in the second, approximately equal proportions of electrons and positrons would be generated. This question was answered by Hildebrand and Meyer in the 1960's through the construction of the first balloon-borne magnet spectrometer. This instrument combined a permanent magnet with optical spark chambers as track detectors and a tantalum-plate spark chamber for electron identification [DeShong 1964]. It could then be shown that the positron fraction in the energy region from 1 to 10 GeV was only of the order of a few percent [Fanselow 1969], and hence, that the majority of the electron component of the cosmic rays at these energies must be of primary origin.

To extend the electron/positron measurements to higher energies, a more powerful magnet spectrometer is required, and the apparatus must exhibit exceptional rejection power against protons (which may outnumber the positrons by a factor of about 10^4). Initial observations in the 1980's, one of which used the earth's magnetic field as a spectrometer [Müller 1987], had reported a sharp increase in the positron fraction above 10 GeV(see Fig. 30).This result could later not be fully verified, but it motivated several groups to attempt new measurements, initially with balloons, and later in space.

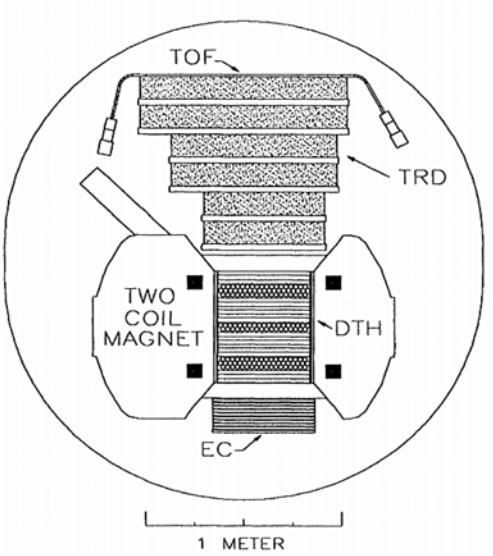

Fig. 31. Schematic cross section of the HEAT-electron spectrometer. This instrument combines the magnet/drift tube hodoscope (DTH) system with shower colorimeter (EC) and transition radiation detector (TRD) for independent electron identification. (Figure from [Barwick 1997a]).

Clearly, if there was a positron excess beyond what could be expected from interstellar secondary production, some other and possibly highly interesting production mechanism would be required. Numerous processes, from electron/positron pair production near pulsars to dark-matter annihilations were proposed.

For new observations of electrons and positrons, the development of the magnet spectrometer technology was essential. Of course, these spectrometers were also used for measurements of the energy spectra and for isotopic analysis of cosmic-ray nuclei (see Sects. 2.6 and 2.7), and for the detection of anti-protons (see Sect. 3.2). The pioneering superconducting magnet developed by the Alvarez-group in Berkeley [Smith 1972] consisted of a single vertical coil, and cosmic-ray particles, moving essentially in directions perpendicular to the axis of the coil, were deflected in a fairly non-uniform magnetic field. Upon the initiative of R. Golden, a collaboration of several US and European institutions has used this type of a magnet spectrometer in a sequence of balloon flights in the 1980s and 1990s (e.g., [Boezio 1997; Golden 1996; Mitchell 1996]). In a program named WIZARD, this group has combined a variety of tracking detectors and particle identifiers, including a ring-imaging Cherenkov counter, imaging calorimetry, and a transition radiation detector, with the superconducting magnet coil.

An alternate approach was to use a classical two-coil superconducting magnet which generates a more uniform magnetic field. Instruments of this type included SMILI [Ahlen 2000], and ISOMAX [Hams 2004] which were designed to resolve light isotopes. For the observation of electrons and positrons, the HEAT spectrometer [Barwick 1997a] was developed (and later modified for anti-proton studies). HEAT also exhibits a two-coil superconducting magnet, and is shown in Figure 31. A very different magnet designed by Yamamoto and collaborators employs a large, thin-walled solenoid (see Sect. 3.2 , and Fig. 34). Finally, for the space flights of the PAMELA and AMS detector systems (see discussion below), the complexity and limited cryogenic live time of a superconducting magnet motivated a return to permanent magnet designs.

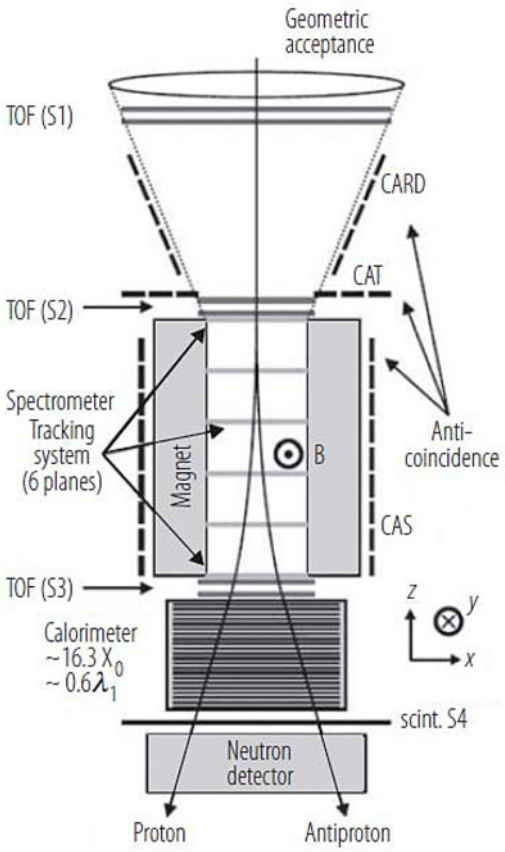

Fig. 32. The PAMELA magnet spectrometer (figure from [Adriani 2009a]). The height of the instrument is about 1.3m. Schematically shown are the trajectories of a proton and an antiproton, with opposite deflections in the magnetic field. The chance for a proton to interact in the electromagnetic calorimeter is small, in contrast to electrons and positrons which always produce showers. The lateral and longitudinal structure of an electron shower is generally quite different from that of the beginning of a hadronic cascade caused by an interacting proton.

Several new balloon-borne investigations of positrons were conducted in the 1990's but often remained quite limited in statistics. Among those, the HEAT collaboration reported a small increase in the positron fraction starting just below 10 GeV [Barwick 1997a; Beatty 2004]. The HEAT result was confirmed on the space shuttle by AMS-01 [Aguilar 2007], and solidified with much improved statistics and extending to much higher energies, by the PAMELA space instrument shown in Figure 32 [Adriani 2009b].

A compilation of the currently available data on the positron fraction is shown in Figure 33. The PAMELA results now cover the energy region to more than 100 GeV. Quite recently, also the Fermi-LAT orbiting gamma-ray telescope has reported positron measurements (shown in Fig. 34) at high energy [Ackermann 2012], using the earth's magnetic field as an analyzer. There appears to be a monotonic increase in the positron fraction which is well above the prediction for interstellar secondary production. Clearly, if these results are correct, a new and extraordinary process is required to account for the positron intensity.

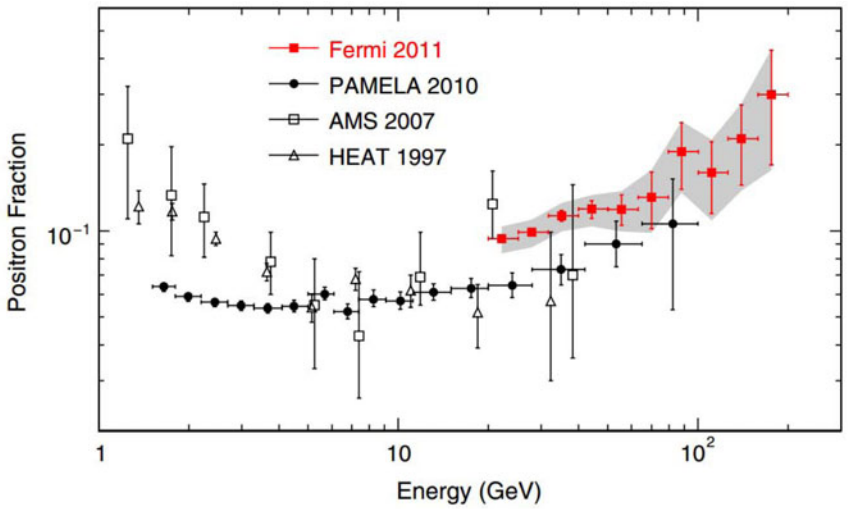

Fig. 33. Positron fraction reported from several recent measurements. The low data points of PAMELA below 10 GeV appear to be depressed due to charge-dependent solar modulation effects (figure from [Ackermann 2012]).

3.2 Anti-protons and anti-nuclei

3.2.1 Anti-protons

Just like positrons, anti-protons must be generated as products of interactions of cosmic-ray protons with hydrogen nuclei in the interstellar gas, provided the proton energy exceeds a threshold of 5.6 GeV. The intensity of antiprotons expected for this process relative to the intensity primary protons (the "pbar/p ratio") is about 10^{-4} around 10 GeV [Gaisser 1997] but is expected to drop rapidly towards lower energies for kinematic reasons. Towards higher energies, a slow decrease is predicted, corresponding to the decrease of the relative abundances of other secondary components such as the light nuclei (see Sect. 2.7.2). Any pbar/p excess over these expectations would indicate the existence of other and possibly exotic sources of antiprotons.

The expected relative abundance of antiprotons is of the same order of magnitude or lower than the abundance of positrons. Therefore, a similar background rejection problem exists for observations. In particular, negative pions produced by cosmic rays in the atmosphere or in the detector material itself, may masquerade as antiprotons. Initial experiments to detect antiprotons in balloon borne investigations were made around 1980, using either magnet spectrometers [Bogomolov 1979; Golden 1979] or trying to observe annihilation stars [Buffington 1981]. These investigations reported significantly higher intensities than expected, and could not be confirmed in later observations. Hence, these measurements were most likely affected by unidentified background.

The first undisputed detection of anti-protons was accomplished in the 1990's with three different superconducting magnet spectrometers on balloons, called BESS [Moiseev 1997; Yoshimura 1995], IMAX [Mitchell 1996] and CAPRICE [Boezio 1997]. The BESS instrument, with its very large horizontal superconducting solenoid, has been repeatedly modified, and has measured the energy spectrum of antiprotons with high precision from 0.1 to ∼40 GeV [Abe 2011]. The instrument is shown in Figure 34.

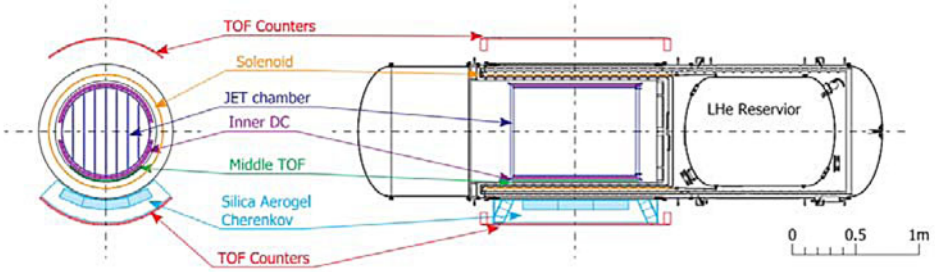

Fig. 34. Cross section and side view of the BESS-Polar II spectrometer. Note the large cylindrical cavity inside the toroidal superconducting magnet which contains particle tracking deters (figure from [Abe 2012]).

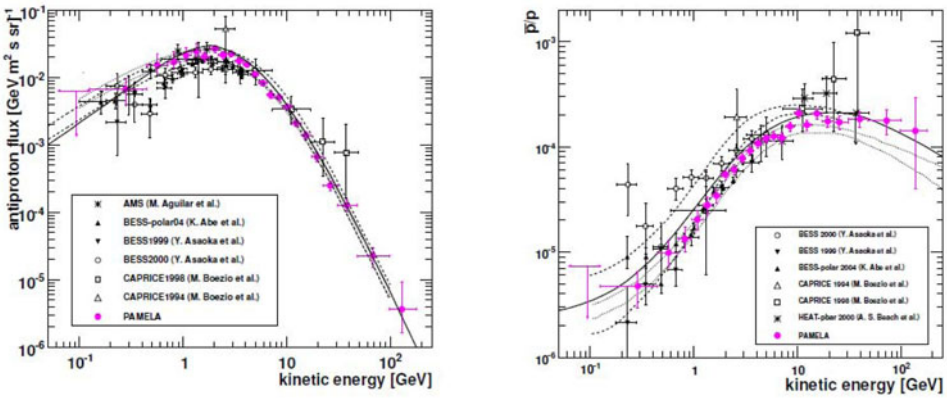

Fig. 35. Left Panel: anti-proton energy spectra. Right Panel: the pbar/p intensity ratio vs. energy. The lines correspond to predictions for secondary interstellar origin of anti-protons at different solar modulation levels (figure from [Wu 2011]).

Including the results of other balloon instruments, e.g. HEAT-pbar [Beach 2001], and two measurements in space with AMS-01 [Aguilar 2002], and with PAMELA [Wu 2011], the pbar/p ratio is now well measured up to about 100 GeV. A compilation of results is shown in Figure 35 [Wu 2011]. The data are in good agreement with the predicted antiproton intensity from interstellar cosmic-ray interactions, and no indication for any unusual or exotic contribution can be found.

3.2.2 Anti-nuclei

The cross sections for the production of anti-nuclei heavier than protons in interstellar p-p collisions are so small that it would be extremely unlikely to observe such particles among the secondary cosmic rays. Rather, if indeed a heavy anti-nucleus were found in the cosmic rays, it would almost certainly imply that there are anti-matter domains in the universe where the anti-nuclei are generated by nucleosynthesis in anti-stars (only anti-helium or anti-deuterons could come from an earlier cosmological epoch). That such stars or anti-matter islands exist in the vicinity (at the scale of about 100 Mpc) of our Galaxy has been essentially ruled out by the lack of observational evidence for gamma radiation from matter-antimatter annihilations [Adams 1997; Cohen 1998].

Nevertheless, the tantalizing question of baryon asymmetry in the universe has motivated a number of searches for cosmic-ray anti-nuclei since the 1970's. Again,

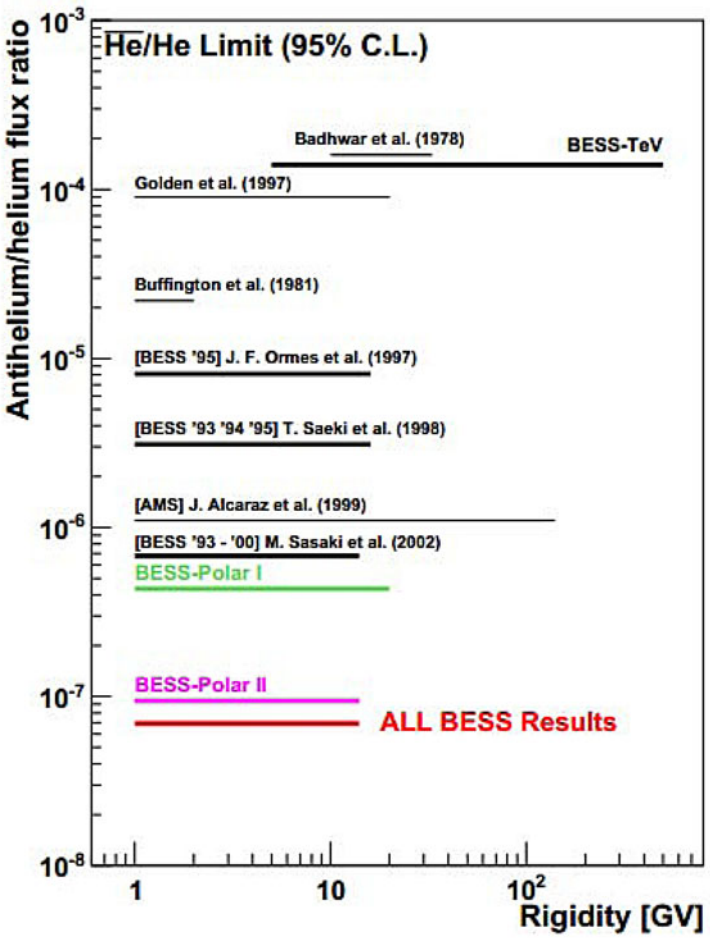

Fig. 36. Upper limits on the relative abundance of anti-alpha particles, reported in several investigations (figure from [Abe 2012], see references therein).

magnet spectrometers were used on balloons and in space, and were mostly focused on searches for anti-helium. Not a single heavy anti-nucleus has been found. The most recent investigations were made with the space shuttle flight of AMS-01 [Alcaraz 1999], the space mission PAMELA [Mayorov 2011], and the BESS balloon experiment [Sasaki 2008]. BESS has now reported upper limits well below 10^{-7} on the intensity ratio of anti-helium to helium. Figure 36 illustrates how the upper limit of the measurements has continually decreased, from about 10^{-4} in the late 1970's to the current result from BESS [Abe 2012].

Upper limits on the relative abundances of heavier nuclei are less stringent; unpublished work from the AMS-01 mission indicates limits in the 10^{-4} to 10^{-5} region.

4 The current view

The variety of investigations that have been conducted over the last half-century in missions on stratospheric balloons or in space is impressive. These direct measurements have provided information on the abundances and energy spectra of the

cosmic-ray components over a great range of species, and at a level of detail which cannot be achieved in indirect air shower observations at the highest energies. The energy range of the direct measurements starts below 10^9 eV per particle, and extends into the 10^{14} to 10^{15} eV per particle region for the more abundant species. The information now available is starting to provide some key answers to the century-old question of the origin of the cosmic rays.

The observations, together with complementary measurements of the electromagnetic radiations, in particular in the gamma-ray region, show that the cosmic-ray particles are a relativistic gas contained within the volume of the Galaxy, including a Galactic halo. The thickness of the halo is not well determined but may be of the order of a few thousand parsec. In the galactic disc, there seems to be roughly equipartition between the energy densities of cosmic rays, of the interstellar gas, of the galactic magnetic fields, and of the cosmic microwave background Cox [2005]. Thus, the pressure of the cosmic-ray gas significantly contributes to the dynamics of the Galaxy. The cosmic-ray particles are tightly confined to the interstellar magnetic field B. The gyration radii are small as compared to galactic dimensions: with the convenient expression $r(\text{parsec}) \approx 10^{-6}\ pc/ZB$ (pc in GeV, B in μG), one finds that a proton of 300 GeV has a gyroradius of just 10^{-4} parsec in a magnetic field of 3 μG. While there is no direct evidence for a *purely* Galactic nature of cosmic rays (except for electrons which cannot traverse inter-galactic distances because of radiative energy losses in the microwave background), it seems unlikely for energetic reasons that the bulk of the cosmic-ray intensity could be universal. Accelerators ("sources") of the cosmic-ray particles are assumed to be located along the plane of the Galaxy, and most likely include supernova remnants.

Key for understanding the details of the acceleration process is the study of galactic propagation, i.e., of the interactions of cosmic rays in the interstellar medium which may affect the composition and energy spectra of the ambient particle population. As a consequence, the spectra and composition of the particles observed near Earth are different from those in the cosmic-ray source. A recent review of these issues has been given by Strong et al. [Strong 2007].

It is common to assume that the differential intensity (i.e., intensity per energy interval) of a particular component is determined by diffusive equilibrium between production and loss of that component in the Galaxy. The major production processes are acceleration in primary sources, and secondary production by nuclear spallation or other interactions of parent particles in interstellar space. Loss processes include spatial diffusion and convection, and eventual escape from the Galaxy, energy gains (re-acceleration) or energy losses, losses by nuclear spallation, and possibly by radioactive decay. A "transport equation" which gives a mathematical description of these processes in the form of a continuity equation, has been formulated long ago by Ginzburg [Ginzburg 1964]. However, the uncertainties in the parameters appearing in the equation are much too large as to permit an analytical solution. The difficulties are particularly severe at the lower energies (below a few GeV per amu) where ionization energy loss during propagation becomes significant, and where the effects of solar modulation greatly complicate the picture.

A popular approximation which gives a reasonable description of the intensities of the more abundant stable cosmic ray nuclei above the energy regime of solar modulation, is the "leaky box model". More detail can be derived from a numerical integration in a diffusion model when the model parameters such as diffusion coefficient and geometric boundary conditions, are adjusted to match the measured data. The GALPROP code [Strong 1998] has been particularly successful in finding a self-consistent description of measured data.

In the leaky-box approximation, the diffusion is parameterized by introducing the average propagation path length $\Lambda(E)$ which is inversely proportional to the diffusion

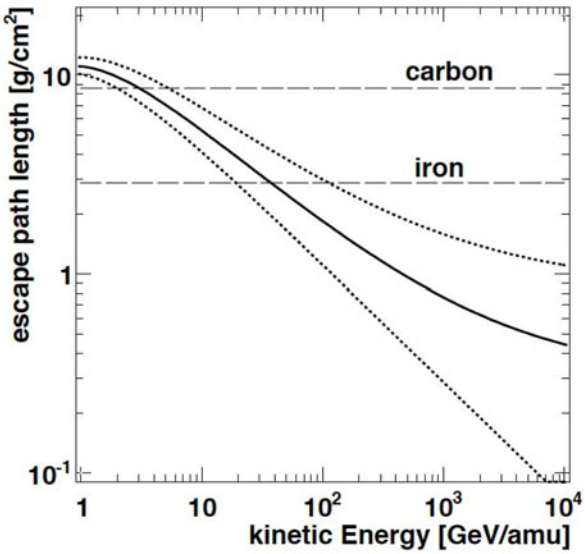

Fig. 37. The escape path length Λ as function of energy. The solid line is fit to the measurements of Figure 22, and the dotted lines represent the uncertainty in the fit. The horizontal dashed lines indicate the interaction lengths of carbon and iron nuclei, respectively (figure from [Obermeier 2012]).

coefficient and may depend on energy:

$$\Lambda(E) = \beta c \rho \tau(E).$$

Here, $\tau(E)$ is the average containment time (or life time) of cosmic rays in the Galaxy, $\beta c = v$ is the particle speed, and ρ the mass density of interstellar gas. At high energy, Λ decreases with energy, as seen in the energy dependence of the intensities of secondary cosmic rays described in Section 2.7.2., and as shown in Figure 37.

For the loss of the particle by spallation reactions with interstellar gas nuclei of mass M, one may introduce a spallation path length $\Lambda_s(A)$:

$$\Lambda_s(A) = \frac{M}{\sigma(A)}.$$

The spallation cross section $\sigma(A)$ depends on the mass number A, but is taken to be independent of energy above a few GeV per nucleon. Example values for carbon and iron nuclei are shown in Figure 37.

The parameters Λ and Λ_s quantify the competition between diffusion and escape in the fate of a cosmic-ray particle. Both parameters may be of similar order of magnitude, but one of them (Λ) depends on energy, while the other (Λ_s) does not. Hence, the energy dependence of the observed spectrum will not be the same as that of the source spectrum: if the source spectrum is a power law in energy $E^{-\alpha}$, the observed spectrum can only have approximate power law form and must be softer than the source spectrum. A detailed analysis of measured data [Ave 2009; Obermeier 2012] has shown that the differential energy spectra of the major heavy primary cosmic-ray nuclei, in the range 20 to 1000 GeV per nucleon, can be approximated with a spectral shape $E^{-\Gamma}$ with $\Gamma = 2.65 \pm 0.05$, while the corresponding source spectrum would have a spectral index $\alpha = 2.3$–2.4. Qualitatively, the same conclusion is also obtained from numerical integration of the diffusion equation with the GALPROP code

[Obermeier 2012]. Comparison of this empirically determined shape of the cosmic-ray source spectrum with the predictions of shock-acceleration theory is a subject of ongoing research. As mentioned in Section 2.7.2, the theory also predicts that shock acceleration ceases to be efficient at high rigidities, of the order $Z \times 10^{14} V$ [Lagage 1983], and that therefore at the corresponding high energies, the composition of the cosmic rays should change. Such changes have not yet convincingly been observed in direct measurements.

Knowing the propagation effects that determine the relation between observed and source spectrum, one may calculate the relative abundances of the elements in the cosmic-ray source and compare this with the "universal" abundance scale mentioned in Section 2.4. (e.g. Ave et al. [Ave 2009]). The somewhat perplexing result of this comparison is that cosmic-ray species with high first ionization potential (FIP), or, alternatively, species with high volatility (low condensation temperature), are relatively under-abundant in the cosmic rays. These correlations, which appear to exist at all energies, are not well understood. The FIP-abundance correlation has also been observed for energetic particles produced in solar flares. This led to the suggestion that the cosmic-ray source material is enriched with particles from stellar atmospheres at temperatures around 10^4 K [Meyer 1997; Webber 1997]. If however, volatility is the valid order parameter, one has to realize that low-volatility elements tend to be frozen out as dust grains in the interstellar medium. Hence, it may be that ionized dust grains are preferentially accelerated to provide the seeds for cosmic-ray particles [Meyer 1997]. As volatility and FIP are correlated for most elements, one cannot easily distinguish between these two alternative models, except for very specific ultra-heavy elements for which this correlation is broken [Link 2003]. Composition measurements for these elements with the required accuracy are not yet available.

These subtle effects may govern the "injection" of individual elements into the cosmic-ray accelerator, but they do not detract from the general picture that the bulk of the cosmic-ray matter has its origin in the interstellar gas and dust of the Galaxy. Isotopic composition measurements such as those of the Fe and Ni isotopes (see Sect. 2.6) indicate that material freshly produced in a supernova explosion would be too young to contribute significantly to the cosmic-ray material. On the other hand, the age of the cosmic-ray particles (around 10^7 years at GeV energies) is much younger than the presumed age of the ISM. The relative isotopic abundances of the primary cosmic rays (which are not affected by chemical fractionation) are nearly identical to the universal abundance scale, except for a small enhancement of ^{58}Fe, and a significant overabundance of ^{22}Ne [Israel 2005]. These findings may be explained if one assumes that supernova shocks provide the dominant acceleration process, but that many supernovae occur in OB associations which contain massive stars (e.g. Wolf-Rayet stars) which have matter outflows enriched in ^{22}Ne and also lead to an enhanced ^{58}Fe/^{56}Fe abundance ratio [Higdon 2003].

Over the years, many searches for exotic particles in the cosmic rays, such as free quarks, magnetic monopoles, mini black holes, dark matter candidates, and anti-nuclei, have been undertaken. None of these has yet been successful. There have occasionally been reports of irregularities or "features" in the energy spectra of cosmic-ray particles. However, often these observations were either statistically not significant, or could not be confirmed by independent observations.

However, one observation currently stands out clearly against any explanation by standard astrophysical phenomena: the increase in the positron fraction at high energy as described in Section 3.1. Many attempts at explanation of this result have been made, perhaps the most exciting suggesting the generation of electron-positron pairs as a consequence of the annihilation of neutralinos ("WIMPs") which have been proposed as carriers of the dark matter in the universe [Turner 1990]. Clearly, independent

observations, and an extension of the energy range of the positron measurements, are required to reach a firm conclusion on this potentially far-reaching issue.

5 Future prospects

Looking towards the future, there are clear observational objectives that need to be addressed in direct measurements in order to resolve the century-old cosmic-ray enigma. These include the confirmation and extension of the positron measurements mentioned above, the shape of the energy spectrum of electrons in the TeV energy region, details of the composition and spectral shape of cosmic-ray nuclei up to the energy region of the "knee" above 10^{15} eV in the "all-particle energy spectrum", and statistically significant measurements of the abundances of ultra-heavy nuclei. New measurements may also address an area not covered in this report, namely continued observations of the energetic particle population in the solar system.

New electron-positron measurements are expected to result from the AMS mission. AMS [Bourquin 2005] is a large and very sophisticated detector system, employing a high-resolution magnet spectrometer, which was launched by the Space Shuttle in 2011 and mounted on the international space station (ISS) after a prototype flight (AMS-01) on the Space Shuttle in 1998. There is currently no other cosmic-ray instrument of comparable magnitude in space orbit. A smaller instrument to detect high-energy electrons (CALET, for $e^+ + e^-$, a successor to the Japanese BETS project on balloons) is in preparation for placement on the Japanese module of ISS [Torii 2004]. In addition, the Fermi gamma-ray telescope and PAMELA are currently active. While Fermi is optimized for the observation of gamma rays, as shown in Section 3.1, it also reports information on the spectrum of electrons. Thus, together with ongoing observations on long-duration balloon (including CREST, an instrument designed to identify high-energy electrons via their emission of synchrotron photons in the earth's magnetic field [Coutu 2011]), additional electron and positron data will become available relatively soon, and hopefully resolve some of the exciting issues connected with electron-observations.

Observations of nuclei up to the knee energy region not only provide detail on cosmic-ray acceleration mechanisms, including constraints on the high-energy limit of the shock acceleration process. Such observations also should overlap with the range of indirect air shower measurements. This would provide a much-needed calibration of the air shower technique which is the only technique available to obtain information up the highest energies in the 10^{20} eV region. However, neither currently active detectors for long-duration balloon flight nor the AMS mission will be able to cover the energy region around the "knee". To accomplish this, a new generation of instruments is required, and should preferably be flown in space. Such missions have been repeatedly proposed, but none is currently in development. Similarly, the composition of super-heavy nuclei is currently being studied in long-duration balloon flight (with the Super-TIGER instrument [de Nolfo 2009]), but in order to reach the counting statistics required for the actinide region, satellite instrumentation is required but not currently available.

Thus, to conclude, a substantial amount of information about the cosmic rays has been collected in direct measurements over the last several decades, and important new data will become available in the coming years. However, not all remaining questions will be answered soon, and one must expect that cosmic-ray research will remain active and exciting well into the second century after Hess' discovery.

Acknowledgements. The author gratefully acknowledges the critical reading of this manuscript by several colleagues. Nevertheless, he is solely responsible for omissions or

misrepresentations that may have occurred. He also thanks Jacob Clementi for help in editing this manuscript.

References

Abe, K. et al. 2011. Measurement of the cosmic-ray antiproton spectrum at solar minimum with a long-duration balloon flight over Antarctica. arXiv:1107.6000

Abe, K. et al. 2012. Search for Antihelium with the BESS-Polar Spectrometer. arXiv:1201.2967v1

Ackermann, M. et al. 2010. Fermi LAT observations of cosmic-ray electrons from 7 GeV to 1 TeV. *Phys. Rev. D* **82**: 092004

Ackermann, M. et al. 2012. Measurement of separate cosmic-ray electron and positron spectra with the Fermi Large Area Telescope. *Phys. Rev. Lett.* **108**: 011103

Adams, F.C. et al. 1997. Constraints on the intergalactic transport of cosmic rays. *Astrophys. J.* **491**: 6-12

Adriani, O. et al. 2009a. The PAMELA space mission. *Nucl. Phys. B* (Proc. Suppl.) **188**: 296-298

Adriani, O. et al. 2009b. An anomalous positron abundance in cosmic rays with energies 1.5-100 GeV. *Nature* **458**: 607-609

Adriani, O. et al. 2011a. The Cosmic-ray electron flux measured by the PAMELA experiment between 1 and 625 GeV. *Phys. Rev. Lett.* **106**: 201101

Adriani, O. et al. 2011b. PAMELA measurements of cosmic-ray proton and helium spectra. *Science* **332**: 69-72

Aguilar, M. et al. 2002. The alpha magnetic spectrometer (AMS) on the international space station: Part I results from the test flight on the space shuttle. *Phys. Rep.* **366**: 331-405

Aguilar, M. et al. 2007. Cosmic-ray positron fraction measurement from 1 to 30 GeV with AMS-01. *Phys. Lett. B* **646**: 145-154

Aharonian, I. et al. 2008. Energy spectrum of cosmic-ray electrons at TeV energies. *Phys. Rev. Lett.* **101**: 261104

Ahlen, S.P. et al. 2000. Measurement of the isotopic composition of cosmic-ray helium, lithium, beryllium, and boron up to 1700 MeV per atomic mass unit. *Astrophys. J.* **534**: 757-769

Ahn, H.S. et al. 2007. The cosmic ray energetics and mass (CREAM) instrument. *Nucl. Instrum. Methods Phys. Res. A* **579**: 1034-1053

Ahn, H.S. et al. 2008. Measurements of cosmic ray secondary nuclei at high energy by the first flight of the CREAM balloon-borne experiment. *Astropart. Phys.* **30**: 133-141

Ahn, H. S. et al. 2010. Discrepant hardening observed in cosmic-ray elemental spectra. *Astrophys. J.* **714**: L89-L93

Alcaraz, J. et al. 1999. Search for antihelium in cosmic rays. *Phys. Lett. B* **461**: 387-396

Alcaraz, J. et al. 2000. Leptons in near earth orbit. *Phys. Lett. B* **484**: 10-22

Alfven, H. 1950. On the solar origin of cosmic radiation. *Phys. Rev.* **77**: 375-379

Alvarez, L. and A.H. Compton. 1933. A positively charged component of cosmic rays. *Phys. Rev.* **43**: 835-836

Amsler, C. et al. 2008. Review of particle physics. *Phys. Lett. B* **667**: 1

Anand, K.C. and R.R. Daniel. S.A. Stephens. 1975. Energy-spectrum of cosmic-ray electrons between 10 and 1000 GeV. *Astrophys. Space Sci.* **36**: 169-175

Anders, E. and M. Ebihara. 1982. Solar-system abundances of the elements. *Geochim. Cosmochim. Acta* **46**: 2363-2380

Apanasenko, A.V. et al. 2001. Composition and energy spectra of cosmic-ray primaries in the energy range 10^{13}–10^{15} eV/particle observed by Japanese-Russian joint balloon experiment. *Astropart. Phys.* **16**: 13-46

Asakimori, K. et al. 1998. Cosmic-ray proton and helium spectra: Results from the JACEE experiment. *Astrophys. J.* **502**: 278-283

Ave, M. at al. 2008. Composition of primary cosmic-ray nuclei at high energies. *Astrophys. J.* **678**: 262-273

Ave, M. et al. 2009. Propagation and source energy spectra of cosmic ray nuclei at high energies. *Astrophys. J.* **697**: 106-114

Ave, M. et al. 2011. The TRACER instrument: A balloon-borne cosmic-ray detector. *Nucl. Instrum. Methods Phys. Res. A* **654**: 140-156

Axford, W.I., E. Leer and G. Skadron. 1977. *Proc. 15th Int. Cosm. Ray Conf., Plovdiv*, Vol. 11, p. 132

Baade, W. and F. Zwicky. 1934a. Supernovae and cosmic rays. *Phys. Rev.* **45**: 138

Baade, W. and F. Zwicky. 1934b. Remarks on super-novae and cosmic rays. *Phys. Rev.* **46**: 76-77

Barwick, S.W. et al. 1997a. Measurements of the cosmic-ray positron fraction from 1 to 50 GeV. *Astrophys. J.* **482**: L191-L194

Barwick, S.W. et al. 1997b. The high-energy antimatter telescope (HEAT): an instrument for the study of cosmic-ray positrons. *Nucl. Instrum. Methods Phys. Res. A* **400**: 34-52

Beach, A.S. et al. 2001. Measurement of the cosmic-ray antiproton-to-proton abundance ratio between 4 and 50 GeV. *Phys. Rev. Lett.* **87**: 271101

Beatty, J.J. et al. 2004. New measurement of the cosmic-ray positron fraction from 5 to 15 GeV. *Phys. Rev. Lett.* **93**: 241102

Bell, A.R. 1978. Acceleration of cosmic-rays in shock fronts. *MNRAS* **182**: 147-156

Binns, W.R. et al. 1981a. Cosmic-ray abundances of elements with atomic-number $26 \leq Z \leq 40$ measured on HEAO-3. *Astrophys. J.* **247**: 115-118

Binns, W.R. et al. 1981b. The UH-nuclei cosmic-ray detector on the 3rd high-energy-astronomy-observatory. *Nucl. Instrum. Methods* **185**: 415-426

Binns, W.R. et al. 1989. *AIP Conf. Proc.* **183**: 147

Blandford, R.D. and J.P. Ostriker. 1978. Particle acceleration by astrophysical shocks. *Astrophys. J.* **221**: L29-L32

Boezio, M. et al. 1997. The cosmic-ray antiproton flux between 0.62 and 3.19 GeV measured near solar minimum activity. *Astrophys. J.* **487**: 415-423

Boezio, M. et al. 2000. The cosmic-ray electron and positron spectra measured at 1 AU during solar minimum activity. *Astrophys. J.* **532**: 653-669

Bogomolov, E.A. et al. 1979. *Proc. 16th Int. Cosm. Ray Conf., Kyoto*, Vol. 1, p. 330

Bouffard, M. et al. 1982. The HEAO-3 cosmic-ray isotope spectrometer. *Astrophys. Space Sci.* **84**: 3-33

Bourquin, M. et al. 2005. The AMS tracking detector for cosmic-ray physics in space. *Nucl. Instrum. Methods Phys. Res. A* **541**: 110-116

Bradt, H.L. and B. Peters. 1948. Investigation of the primary cosmic radiation with nuclear photographic emulsions. *Phys. Rev.* **74**: 1828-1837

Buckley, J. et al. 1994. A new measurement of the flux of the light cosmic-ray nuclei at high energies. *Astrophys. J.* **429**: 736-747

Buffington, A., S.M. Schindler and C.R. Pennypacker. 1981. A measurement of the cosmic-ray antiproton flux and a search for anti-helium. *Astrophys. J.* **248**: 1179-1193

Burnett, T.H. et al. 1986. JACEE emulsion chambers for studying the energy-spectra of high-energy cosmic-ray protons and helium. *Nucl. Instrum. Methods Phys. Res. A* **251**: 583-595

Chang, J. et al. 2008. An excess of cosmic ray electrons at energies of 300–800 GeV. *Nature* **456**: 362-365

Clay, J. and H.P. Berlage. 1932. Variation der Ultrastrahlung mit der geographischen Breite und dem Erdmagnetismus. *Naturwiss.* **20**: 687

Cohen, A.G., A. de Rujula and S.L. Glashow. 1998. A matter-antimatter universe? *Astrophys. J.* **495**: 539-549

Compton, A.H. 1932. Variations of cosmic rays with latitude. *Phys. Rev.* **41**: 111-113

Compton, A.H. 1933. A geographic study of cosmic rays. *Phys. Rev.* **43**: 387-403

Coutu, S. et al. 2011. Searching for TeV cosmic electrons with the CREST experiment. *Nucl. Phys. B (Proc. Suppl.)* **215**: 250-254

Cox, D.P. 2005. The three-phase interstellar medium revisited. *Ann. Rev. Astron. Astrophys.* **43**: 337-385

De Shong, J.A., R.H. Hildebrand and P. Meyer. 1964. Ratio of electrons to positrons in primary cosmic radiation. *Phys. Rev. Lett.* **12**: 3-6

Diehl, E. et al. 2003. The energy spectrum of cosmic-ray protons and helium near 100 GeV. *Astropart. Phys.* **18**: 487-500

DuVernois, M.A. et al. 2001. Cosmic-ray electrons and positrons from 1 to 100 GeV: Measurements with HEAT and their interpretation. *Astrophys. J.* **559**: 296-303

Dwyer, R. and P. Meyer. 1981. *Proc. 17th Int. Conf. Cosm. Rays*, Paris, Vol. 2, p. 54

Earl, J. 1961. Cloud-chamber observations of primary cosmic-ray electrons. *Phys. Rev. Lett.* **6**: 125-128

Ellsworth, R.W. et al. 1977. High-energy proton spectrum measurements. *Astrophys. Space Sci.* **52**: 415-427

Engelmann, J.J. et al. 1981. *Proc. 17th Int. Cosm. Ray Conf., Paris*, Vol. 9, p. 97

Engelmann, J.J. et al. 1990. Charge composition and energy-spectra of cosmic-ray nuclei for elements from Be to Ni – results from HEAO-3-C2. *Astron. Astrophys.* **233**: 96-111

Fanselow, J.L. et al. 1969. Charge composition and energy spectrum of primary cosmic-ray electrons. *Astrophys. J.* **158**: 771-780

Fermi, E. 1949. On the Origin of the Cosmic Radiation. *Phys. Rev.* **75**: 1169-1174

Ficenec, D.J. et al. 1993. *Proc. 23rd Int. Cosmic Ray Conf., Calgary*, Vol. 1, p. 515

Fleischer, R.L. et al. 1967a. Tracks of heavy primary cosmic rays in meteorites. *JGR* **72**: 355-366

Fleischer, R.L. et al. 1967b. Tracks of cosmic rays in plastics. *Science* **155**: 187-189

Fowler, P.H. et al. 1967 *Proc. Roy. Soc. Lond. A* **301**: 39

Fowler, P.H. et al. 1979. *Proc. 16th Int. Cosm. Ray Conf., Kyoto*, Vol. 12, p. 338

Freier, P. et al. 1948a. Evidence for heavy nuclei in the primary cosmic radiation. *Phys. Rev.* **74**: 213-217

Freier, P. et al. 1948b. The heavy component of primary cosmic rays. *Phys. Rev.* **74**: 1818-1827

Gaisser, T.K. and R.K. Schaefer. 1997. Theoretical predictions for cosmic ray secondary antiprotons. *Adv. Space Res.* **19**: 775-780

Garcia-Munoz, M. and J.A. Simpson. 1979. *Proc. 16th Int. Conf. Cosmic Rays, Kyoto*, Vol. 1, p. 270

Garcia-Munoz, M., G.M. Mason and J.A. Simpson. 1973. Abundances of galactic cosmic-ray carbon, nitrogen, and oxygen and their astrophysical implications. *Astrophys. J.* **184**: 967-994

Garcia-Munoz, M., G.M. Mason and J.A. Simpson. 1975a. Isotopic composition of galactic cosmic-ray lithium, beryllium, and boron. *Astrophys. J.* **201**: 145-148

Garcia-Munoz, M., G.M. Mason and J.A. Simpson. 1975b. Cosmic-ray age deduced from Be-10 abundance. *Astrophys. J.* **201**: 141-144

Ginzburg, V.L. and S. Syrovatskii. 1964. *The Origin of Cosmic Rays*. McMillan, New York

Golden, R.L. et al. 1979. Evidence for the existence of cosmic-ray anti-protons. *Phys. Rev. Lett.* **43**: 1196-1199

Golden, R.L. et al. 1996. Measurement of the positron to electron ratio in the cosmic rays above 5 GeV. *Astrophys. J.* **457**: L103-L106

Grigorov, N.L. et al. 1966. Some problems and perspective in cosmic-ray studies. *Space Sci. Rev.* **5**: 167-209

Grigorov, N.L. et al. 1970. Measurement of effective cross sections of inelastic interaction of protons with carbon and hydrogen nuclei in energy region 20–600 GeV in satellites proton-1, proton-2, and proton-3. *Sov. J. Nucl. Phys.* 11, **455**: 588

Grigorov, N.L. et al. 1971a. *Proc. 12th Int. Cosmic Ray Conf., Hobart*, Vol. 5, p. 1746

Grigorov, N.L. et al. 1971b. *Proc. 12th Int. Cosmic Ray Conf., Hobart*, Vol. 5, p. 1752

Grigorov, N.L. et al. 1971c. *Proc. 12th Int. Cosmic Ray Conf., Hobart*, Vol. 5, p. 1760

Grimani, C. et al. 2002. Measurements of the absolute energy spectra of cosmic-ray positrons and electrons above 7 GeV. *Astron. Astrophys.* **392**: 287-294

Guzik, T.G. et al. 2004. The ATIC Long Duration Balloon project. *Adv. Space Res.* **33**: 1763-1770

Haino, S. et al. 2004. Measurements of primary and atmospheric cosmic-ray spectra with the BESS-TeV spectrometer. *Phys. Lett. B* **594**: 35-46

Hams, T. et al. 2004. Measurement of the abundance of radioactive Be-10 and other light isotopes in cosmic radiation up to 2 GeV per nucleon with the balloon-borne instrument ISOMAX. *Astrophys. J.* **611**: 892-905

Hartmann, G., D. Müller and T. Prince. 1977. High-energy cosmic-ray electrons – a new measurement using transition-radiation detectors. *Phys. Rev. Lett.* **38**: 1368-1372

Hess, V.F. 1912. Ueber Beobachtungen der durchdringenden Strahlung bei sieben Freiballonfahrten. *Physik. Z.* **13**: 1084-1091

Higdon, J.C. and R.E. Lingenfelter. 2003. The superbubble origin of ^{22}Ne in cosmic rays. *Astrophys. J.* **590**: 822-832

Hilberry, N. 1941. Extensive cosmic-ray showers and the energy distribution of primary cosmic rays. *Phys. Rev.* **60**: 1-9

Hulsizer, R.I. and B. Rossi. 1948. Search for electrons in the primary cosmic radiation. *Phys. Rev.* **73**: 1402-1403

Israel, M.H. et al. 2005. Isotopic composition of cosmic rays: Results from the cosmic ray isotope spectrometer on the ACE spacecraft. *Nucl. Phys. A* **758**: 201c-208c.

Ivanenko, I.P. et al. 1988. Energy-spectrum and charge composition of primary cosmic-rays with energy above 2 TeV. *JETP Lett.* **48**: 510-513

Johnson, T.H. and J.C. Street. 1933. The variation of cosmic-ray intensities with azimuth on Mt. Washington, N.H. *Phys. Rev.* **43**: 381

Juliusson, E., P. Meyer and D. Müller. 1972. Composition of cosmic-ray nuclei at high-energies. *Phys. Rev. Lett.* **29**: 445-448

Kobayashi, T. et al. 1999. *Proc. 26th Int. Cosmic Ray Conference*, *Salt Lake City*, Vol. 3, p. 61

L'Heureux, J. et al. 1990. A detector for cosmic-ray nuclei at very high-energies. *NIM A* **295**: 246-260

Lagage, P.O. and C.J. Cesarsky. 1983. The maximum energy of cosmic-rays accelerated by super-nova shocks. *Astron. Astrophys.* **125**: 249-257

Lezniak, J.A. and W.R. Webber. 1978. Charge composition and energy-spectra of cosmic-ray nuclei from 3000 MeV per nucleon to 50 GeV per nucleon. *Astrophys. J.* **223**: 676-696

Link, J.T. et al. 2001. *Proc. 27th Int. Cosm. Ray Conf., Hamburg*, Vol. 6, p. 2143

Link, J.T. et al. 2003. *Proc. 28th ICRC, Tsukuba*, Vol. 4, p. 1781

Linsley, J. 1983. *Proc. 18th Int. Cosmic Ray Conf., Bangalore*, Vol. 12, p. 135

Lodders, K. 2003. Solar system abundances and condensation temperatures of the elements. *Astrophys. J.* **591**: 1220-1247

Lukasiak, A. et al. 1994a. The isotopic composition of cosmic-ray beryllium and its implication for the cosmic-ray's age. *Astrophys. J.* **423**: 426-431

Lukasiak, A. et al. 1994b. Cosmic-ray isotopic composition of C, N, O, Ne, Mg, Si nuclei in the energy-range 50–200 MeV per nucleon measured by the voyager spacecraft during the solar minimum period. *Astrophys. J.* **426**: 366

Lukasiak, A., F. B. McDonald and W. R. Webber. 1994c. Voyager measurements of the isotopic composition of cosmic-ray aluminum and implications for the propagation of cosmic-rays. *Astrophys. J.* **430**: L69-L72

Lukasiak, A. et al. 1997. Voyager measurements of the isotopic composition of Fe, Co and Ni nuclei – Implications for the nucleosynthesis and the acceleration of cosmic rays. *Adv. Space Res.* **19**: 747-750

Mayorov, A.G. et al. 2011. The search for antihelium in cosmic rays using data from the PAMELA experiment. *Bull. Russ. Acad. Sci. Phys.* **75**: 331-333

Meyer, J.P. 1985. Solar-stellar Outer atmospheres and energetic particles, and galactic cosmic rays. *Astrophys. J. Suppl.* **57**: 173

Meyer, P. and R. Vogt. 1961. Electrons in primary cosmic radiation. *Phys. Rev. Lett.* **6**: 193-196

Meyer, J.P., L. O'C. Drury and D.C. Ellison. 1997. Galactic cosmic rays from supernova remnants. A cosmic-ray composition controlled by volatility and mass-to-charge ratio. *Astrophys. J.* **487**: 182-196

Mitchell, J.W. et al. 1993. *Proc. 23rd In. Cosmic Ray Conf., Calgary*, Vol. 1, p. 519
Mitchell, J.W. et al. 1996. Measurement of 0.25–3.2 GeV antiprotons in the cosmic radiation. *Phys. Rev. Lett.* **76**: 3057-3060
Moiseev, A. et al. 1997. Cosmic-ray antiproton flux in the energy range form 200 to 600 MeV. *Astrophys. J.* **474**: 479-489
Müller, D. and K. Tang. 1987. Cosmic-ray positrons from 10 to 20 GeV – a balloon-borne measurement using the geomagnetic east-west asymmetry. *Astrophys. J.* **312**: 183-194
Müller, D. et al. 1991. Energy-spectra and composition of primary cosmic-rays. *Astrophys. J.* **374**: 356-365
Müller, D. 2004. Transition radiation detectors in particle astrophysics. *Nucl. Instrum. Meth. Phys. Res. A* **522**: 9-15
Nishimura, J. et al. 1980. Emulsion chamber observations of primary cosmic-ray electrons in the energy-range 30–1000 GeV. *Astrophys. J.* **238**: 394-409
de Nolfo, G.A. et al. 2009. *Proc. 14th ICRC, Lodz*, unpublished
Obermeier, A. et al. 2011. Energy spectra of primary and secondary cosmic-ray nuclei measured with tracer. *Astrophys. J.* **742**: 14
Obermeier, A. et al. 2012. The boron to carbon abundance ratio and galactic propagation of cosmic radiation. *Astrophys. J.* **752**: 69-75
Panasyuk, M.I. 2011. Cosmic ray physics in space: the role of Sergey Vernov's scientific school. *Astrophys. Space Sci. Trans.* **7**: 151-156
Panov, A.D. et al. 2007. *Proc. 30th ICRC, Merida*, Vol. 2, p. 3
Pfotzer, G. 1936. Dreifachkoinzidenzen der Ultrastrahlung aus vertikaler Richtung in der Stratosphaere. *Z. Phys.* **102**: 23-58
Pomerantz, M.A. and F.L. Hereford. 1949. The detection of heavy particles in the primary cosmic radiation. *Phys. Rev.* **76**: 997-998
Powell, J.C., P.H. Fowler, and D.H. Perkins. 1959. *The Study of Elementary Particles by the Photographic Method*. Pergamon Press
Price, P.B. et al. 1968. High-resolution study of low-energy heavy cosmic rays with lexan track detectors. *Phys. Rev. Lett.* **21**: 630-633
Prince, T.A. 1979. Energy-spectrum of cosmic-ray electrons between 9 and 300 GeV. *Astrophys. J.* **227**: 676-693
Richtmyer, R.D. and E. Teller. 1949. On the origin of cosmic rays. *Phys. Rev.* **75**: 1729-1731
Rossi, B. 1964. *Cosmic Rays*. McGraw Hill
Ryan, M.J. et al. 1972. Cosmic-ray proton and helium spectra above 50 GeV. *Phys. Rev. Lett.* **28**: 985-988
Sasaki, M. et al. 2008. Search for antihelium: Progress with BESS. *Adv. Space Res.* **42**: 450-454
Schein, M., W.P. Jesse and E.O. Wollan. 1941. The nature of the primary cosmic radiation and the origin of the mesotron. *Phys. Rev.* **59**: 615-615
Seo, E.S. et al. 1991. Measurement of cosmic-ray proton and helium spectra during the 1987 solar minimum. *Astrophys. J.* **378**: 763-772
Silverberg, R.F., J.F. Ormes and V.K. Balasubrahmanian. 1973. Primary cosmic-ray electrons above 10 GeV – measurements using a thick detector. *J. Geophys. Res.* **78**: 7165-1773
Silverberg, R.F. 1976. Measurement of primary cosmic electron spectrum from 10 to about 250 GeV. *J. Geophys. Res.* **81**: 3944-3952
Simpson, J.A. 1983. Elemental and Isotopic Composition of the Galactic Cosmic Rays. *Ann. Rev. Nucl. Part. Sci.* **33**: 323-382
Simpson, J.A. et al. 1992. The Ulysses cosmic ray and solar particle investigation. *Astron. Astrophys. Suppl. Ser.* **92**: 365-399
Smith, L.H. et al. 1972. Superconducting magnetic spectrometer for cosmic-ray nuclei. *Rev. Sci. Instrum.* **43**: 1-12
Smith, L.H. et al. 1973. Measurement of cosmic-ray rigidity spectra above 5 GV/c of elements from hydrogen to iron. *Astrophys. J.* **180**: 987-1010
Stone, E.C. et al. 1977. Cosmic-ray investigation for Voyager missions; energetic particle studies in the outer heliosphere and beyond. *Space Sci. Rev.* **21**: 355-376

Stone, E.C. et al. 1998a. The cosmic-ray isotope spectrometer for the advanced composition explorer. *Space Sci. Rev.* **86**: 285-356

Stone, E.C. et al. 1998b. The solar isotope spectrometer for the advanced composition explorer. *Space Sci. Rev.* **86**: 357-408

Strong, A.W. and I.V. Moskalenko. 1998. Propagation of cosmic-ray nucleons in the galaxy. *Astrophys. J.* **509**: 212-228

Strong, A.W. et al. 2007. Cosmic-ray propagation and interactions in the galaxy. *Ann. Rev. Nucl. Part. Sci.* **57**: 285-327

Swordy, S.P. et al. 1990. Relative abundances of secondary and primary cosmic-rays at high-energies. *Astrophys. J.* **349**: 625-633

Tang, K.K. 1984. The energy-spectrum of electrons and cosmic-ray confinement – a new measurement and its interpretation. *Astrophys. J.* **278**: 881-892

Torii, S. et al. 2004. The CALET, CALorimetric Electron Telescope, on ISS/JEM *Nucl. Phys. B (Proc. Suppl.)* **134**: 23-30

Torii, S. et al. 2001. The energy spectrum of cosmic-ray electrons from 10 to 100 GeV observed with a highly granulated imaging calorimeter. *Astrophys. J.* **559**: 973-984

Turner, M.S. and F. Wilczek. 1990. Positron line radiation as a signature of particle dark matter in the halo. *Phys. Rev. D* **42**: 1001-1007

van Allen, J. and H.E. Tatel. 1948. The cosmic-ray counting rate of a single Geiger counter from ground level to 161 kilometers altitude. *Phys. Rev.* **73**: 245-251

Vernoff, S.N. 1934. On the study of cosmic rays at the great altitudes. *Phys. Rev.* **46**: 822-822

Weaver, B.A. and A.J. Westphal. 2002. Extended analysis of the trek ultraheavy collector *Astrophys. J.* **569**: 493-500

Webber, W.R. 1982. Charge abundances of cosmic-rays at their source. *Astrophys. J.* **255**: 329-340

Webber, W.R. 1997. New experimental data and what it tells us about the sources and acceleration of cosmic rays. *Space Sci. Rev.* **81**: 107-142

Wiedenbeck, M.E. and D.E. Greiner. 1980. A cosmic-ray age based on the abundance of Be-10. *Astrophys. J.* **239**: L139-L142

Wiedenbeck, M.E. et al. 1999. Constraints on the time delay between nucleosynthesis and cosmic-ray acceleration from observations of Ni-59 and Co-59. *Astrophys. J.* **523**: 61-64

Wiedenbeck, M.E. et al. 2007. An overview of the origin of galactic cosmic rays as inferred from observations of heavy ion composition and spectra. *Space Sci. Rev.* **130**: 415-429

Wu, J. on behalf of the PAMELA collaboration. 2011. Measurements of cosmic-ray antiprotons with PAMELA. *Astrophys. Space Sci. Trans.* **7**: 225-228

Yanasak, N.E. et al. 2001. Measurement of the secondary radionuclides Be-10, Al-26, Cl-36, Mn-54, and C-14 and implications for the galactic cosmic-ray age. *Astrophys. J.* **563**: 768-792

Yoon, Y.S. et al. 2011. Cosmic-ray proton and helium spectra from the first CREAM flight. *Astrophys. J.* **728**: 122

Yoshimura, K. et al. 1995. Observation of cosmic-ray antiprotons at energies below 500 MeV. *Phys. Rev. Lett.* **75**: 3792-3795

Young, J.S. et al. 1981. The elemental and isotopic composition of cosmic-rays – silicon to nickel. *Astrophys. J.* **246**: 1014-1030